

Time of flight measurements at the FOOT experiment: detector characterization and preliminary results

FACOLTÀ DI SCIENZE
MATEMATICHE, FISICHE E NATURALI



SAPIENZA
UNIVERSITÀ DI ROMA

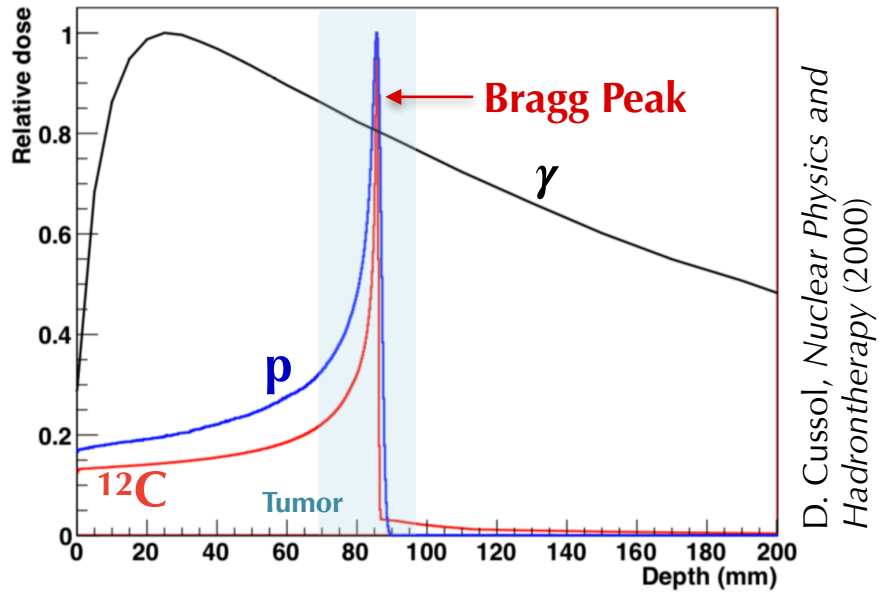
Thesis Advisor: **Prof. Riccardo Faccini**

Co-Advisor: **Prof. Alessio Sarti**

Candidate: **Gaia Franciosini**

Academic Year **2018/2019**

Particle Therapy



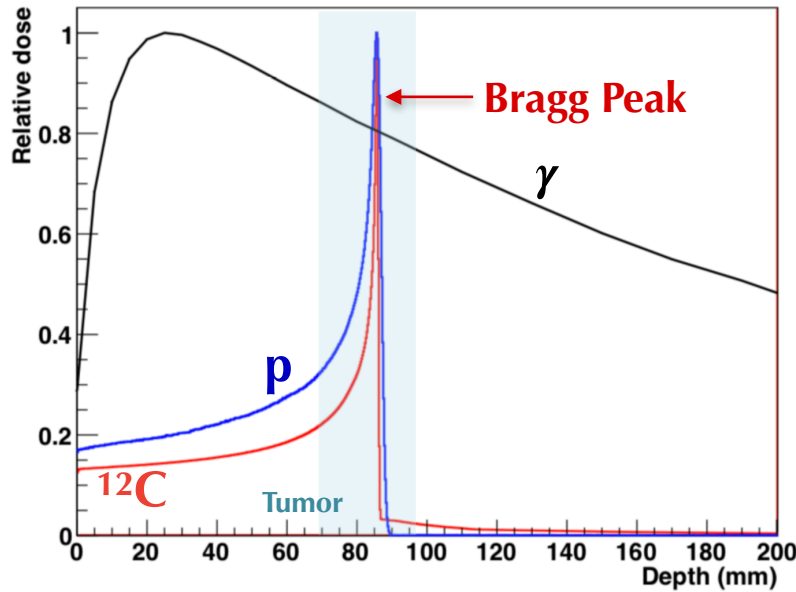
PT vs Conventional Therapy (x-rays):

- ▶ The energy released is highly selective
- ▶ Enhanced Relative Biological Effectiveness (RBE)

$$D = \frac{d\bar{\epsilon}}{dm} \quad [G_y]$$

$$RBE = \frac{D_{ref}(\gamma)}{D_{ion}}$$

Particle Therapy



D. Cussol, Nuclear Physics and Hadrontherapy (2000)

PT vs Conventional Therapy (x-rays):

- ▶ The energy released is highly selective
- ▶ Enhanced Relative Biological Effectiveness (RBE)

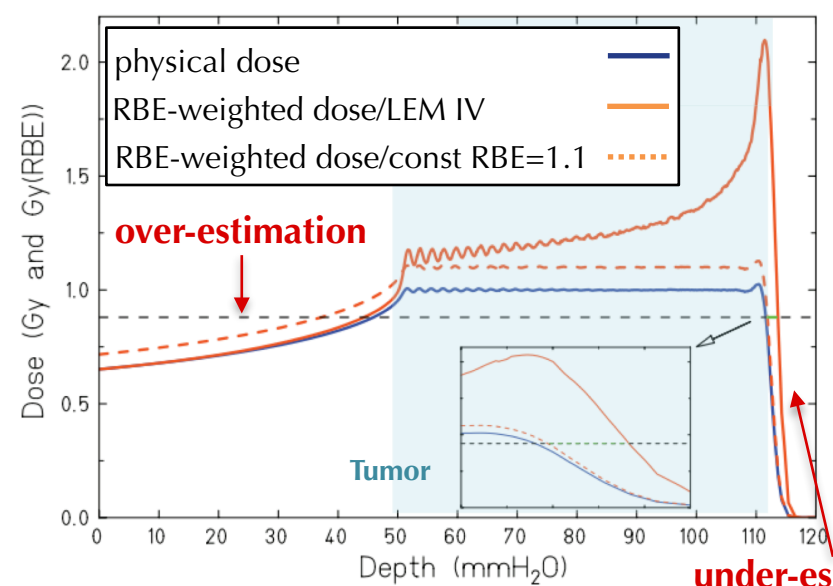
$$D = \frac{d\bar{\epsilon}}{dm} \quad [G_y]$$

$$RBE = \frac{D_{ref}(\gamma)}{D_{ion}}$$

Proton Therapy

In clinical practice protons RBE = 1.1

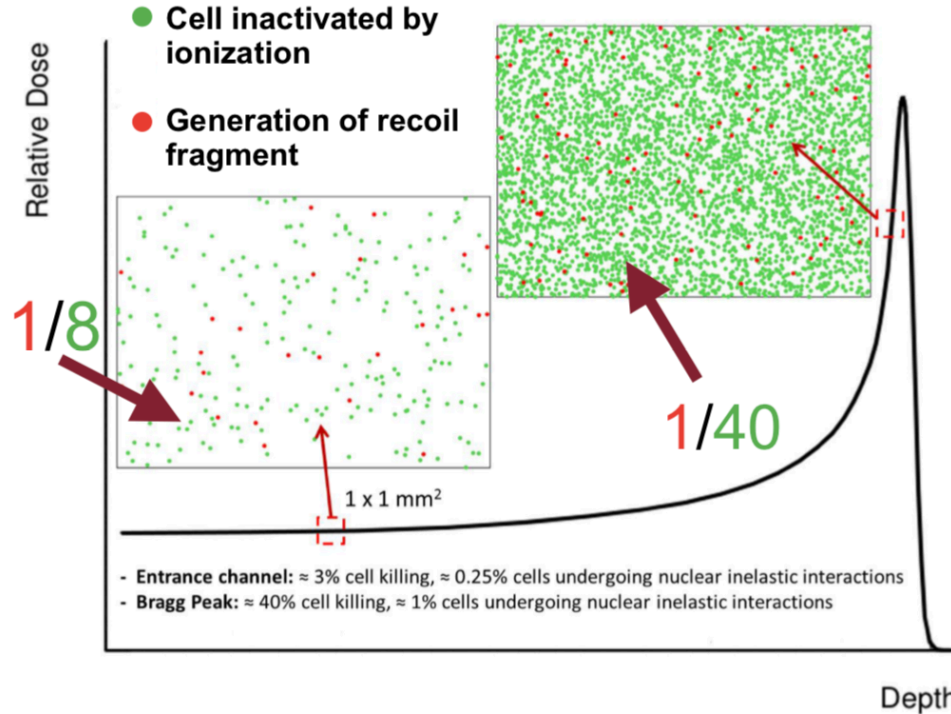
Radiobiological measurements have actually proven that the proton RBE could be over- or under-estimated.



Paganetti H., Relative Biological Effectiveness (RBE) values for proton beam therapy (2014)

under-estimation

Target fragmentation contribution



The particles produced in target fragmentation are one of the causes contributing (~10%) to the increase of proton RBE

$$p + x \rightarrow p + \sum_i x_i$$

▶ $T_{x_i} \ll T_p$ → The fragments have **high RBE values**

▶ $\left(\frac{dE}{dx}\right)_x \gg \left(\frac{dE}{dx}\right)_p$

Very few data

It is essential to improve the knowledge about the role of nuclear fragmentation in proton therapy to improve the treatment planning with a more complete proton RBE model, which include the fragmentations effects.



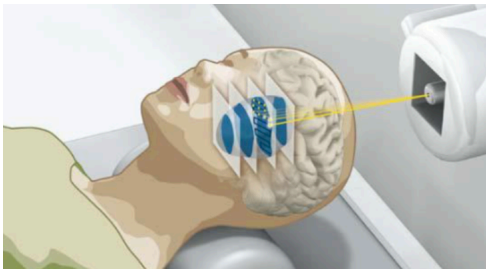
FOOT (FragmentatiOn Of Target) experiment



Measurements of target and projectile fragmentation cross section relevant for **PT** and for **Radio Protection in Space** applications.

Particle Therapy

- ▶ Cross section for therapeutic beams at therapeutic energies:
 - 100-250 MeV for protons
 - 100-350 MeV/u for C ions
 - 100-400 MeV/u for O ions
- ▶ Tissue-like target (H,C,O)



Space radioprotection

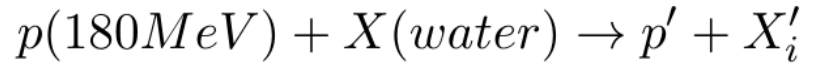
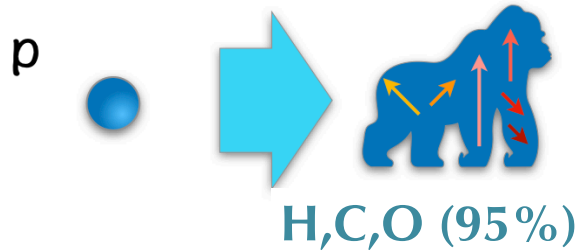
- ▶ Cross section for high energy:
 - 700 MeV/u for He ions
 - 700 MeV/u for C ions
 - 700 MeV/u for O ions
- ▶ H,C,O targets



The accuracy of these measurements is dictated by the requirements sets by the PT radiobiologists → **5%**.

FOOT strategy: inverse kinematic approach

Direct kinematic

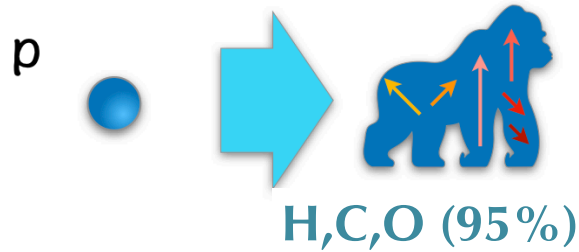


| Fragment | E [MeV] | LET (keV/ μm) | Range (μm) |
|-----------------|---------|---------------------------|-------------------------|
| ^{15}O | 1.0 | 983 | 2.3 |
| ^{15}N | 1.0 | 925 | 2.5 |
| ^{14}N | 2.0 | 1137 | 3.6 |
| ^{13}C | 3.0 | 951 | 5.4 |
| ^{12}C | 3.8 | 912 | 6.2 |
| ^{11}C | 4.6 | 878 | 7.0 |

Target fragments have a very **low energy** and **short range**. Their experimental detection is extremely difficult.

FOOT strategy: inverse kinematic approach

Direct kinematic

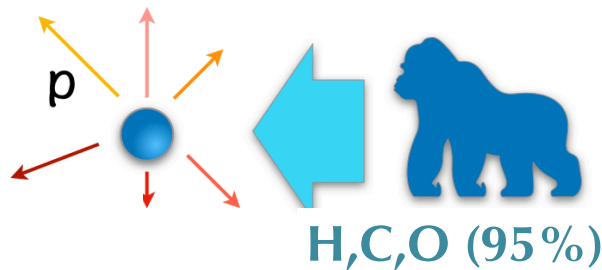


$$p(180\text{MeV}) + X(\text{water}) \rightarrow p' + X'_i$$

| Fragment | E [MeV] | LET (keV/ μm) | Range (μm) |
|-----------------|---------|---------------------------|-------------------------|
| ^{15}O | 1.0 | 983 | 2.3 |
| ^{15}N | 1.0 | 925 | 2.5 |
| ^{14}N | 2.0 | 1137 | 3.6 |
| ^{13}C | 3.0 | 951 | 5.4 |
| ^{12}C | 3.8 | 912 | 6.2 |
| ^{11}C | 4.6 | 878 | 7.0 |

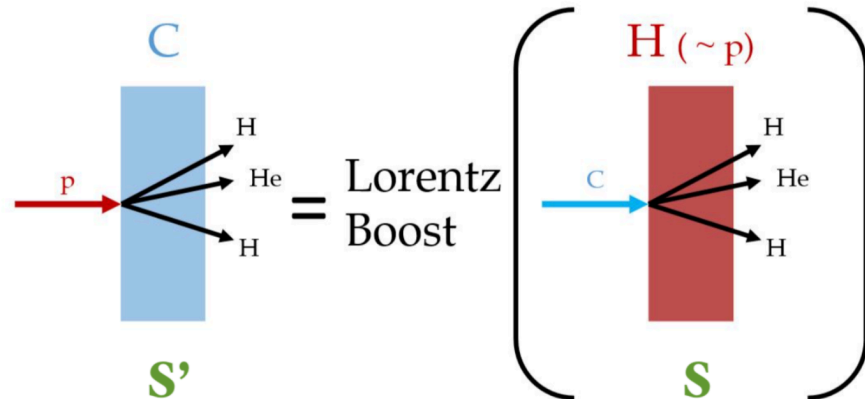
Target fragments have a very **low energy** and **short range**. Their experimental detection is extremely difficult.

Inverse kinematic



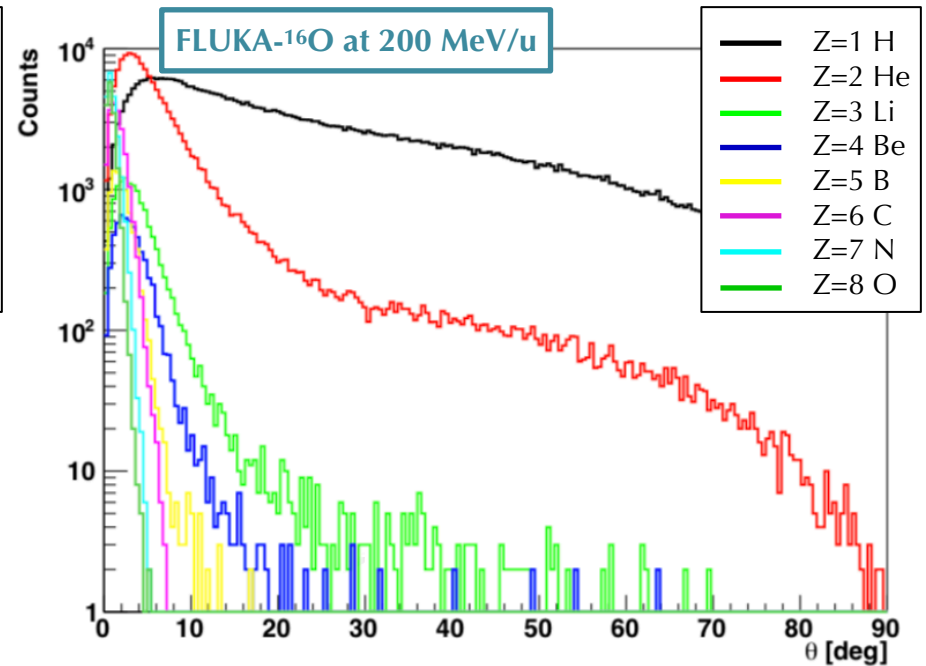
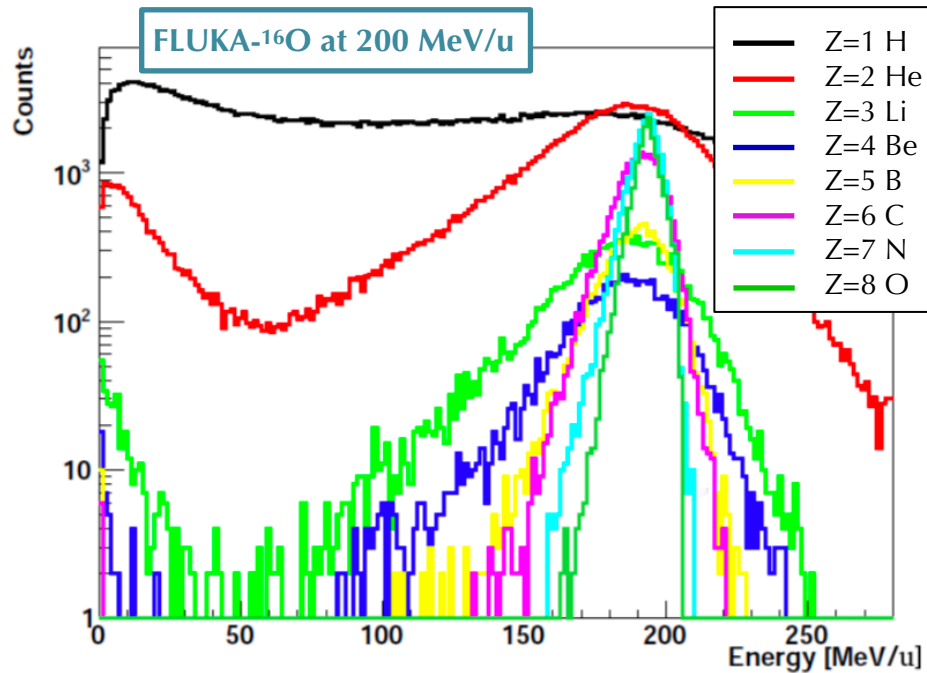
Proton beam on patient-target
(Patient frame of reference)

Patient-target on Proton beam
(Laboratory frame of reference)



➔ In this case the fragments have a longer range and a mean kinetic energy comparable to the projectile one.

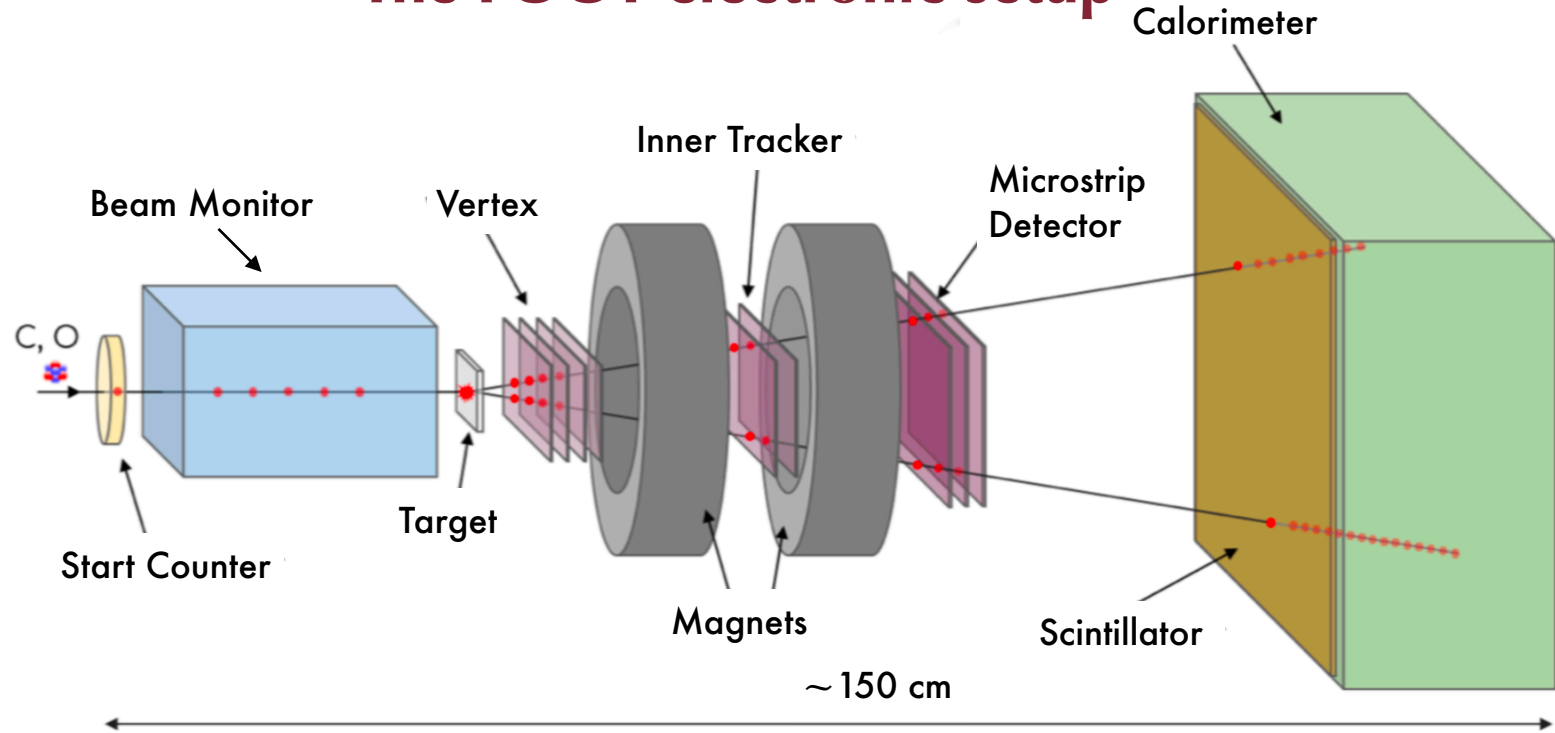
The FOOT experiment setups



The FOOT project includes the development of two different experimental setups:

- ▶ Electronic setup to measure the heavier fragments ($\vartheta < 10^\circ$);
- ▶ Emulsion spectrometer for the lighter ones ($Z \leq 3$), which allows to extend the angular acceptance up to 70° .

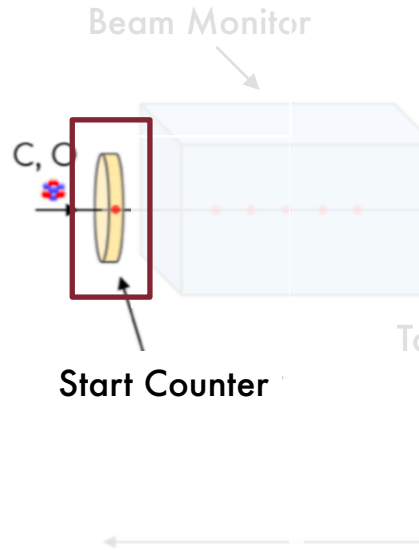
The FOOT electronic setup



Maximum rate ~ 1 kHz due to the low rate capability (few kHz) of the silicon pixel trackers (MIMOSA-28 sensor) & of the scintillator readout that causes a dead time of the order of $100 \mu s$

| | |
|-----------------------------|---------------|
| $\sigma(E)/E$ | 2-3 % |
| $\sigma(p)/p$ | 5 % |
| $\sigma(TOF)$ | ~ 100 ns |
| $\sigma(Z)/Z$ | 2-3 % |
| $\sigma(\Delta E)/\Delta E$ | 3-10 % |

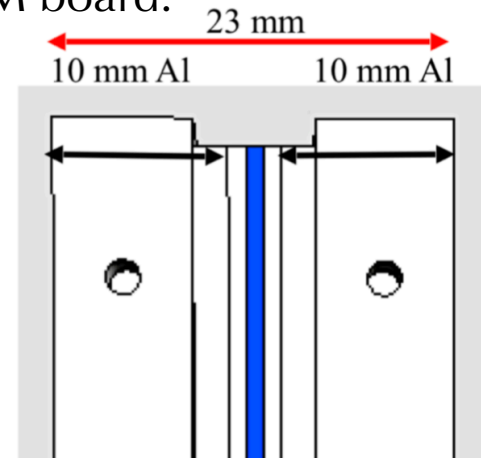
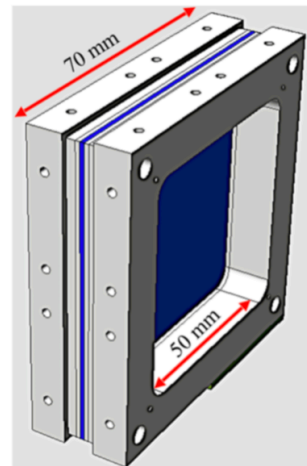
The FOOT electronic setup



The **SC** is a thin (250 μm - 1mm) plastic scintillator layer (EJ-204) placed about 30 cm before the target with an active surface of 5x5 cm².

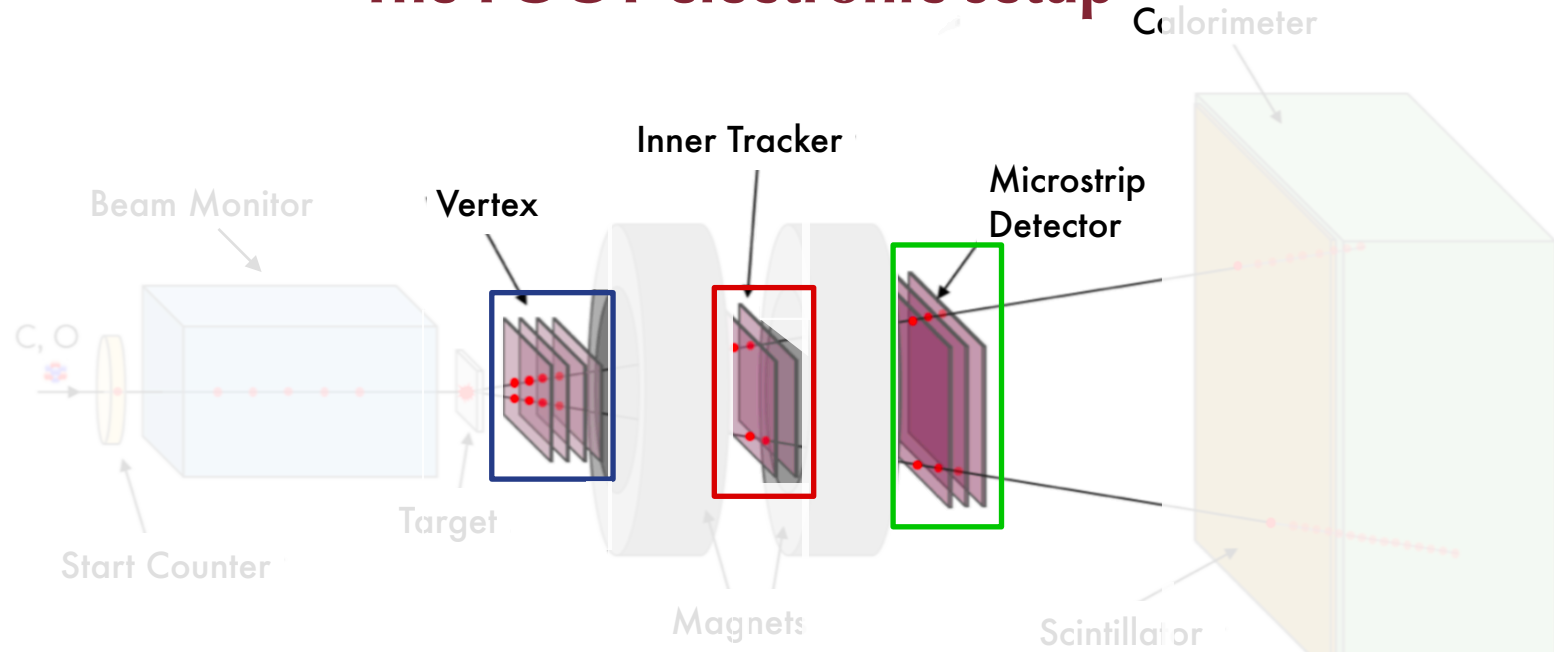
- ▶ Provides the start of the TOF measurements, trigger signal and the measurement of the incoming ion flux (\rightarrow cross section)
- ▶ The SC aims for a time resolution of 60-70 ps (¹²C at 200 MeV/u);
- ▶ The readout (8 channels) and powering of the SiPMs is handled by the WaveDREAM board.*

Maximum rate ~ 1 kHz
 capability (few kHz)
 trackers (MIMOSA-28)
 scintillator readout that
 the order of 100 μs



*Electronic system from MEG II experiment

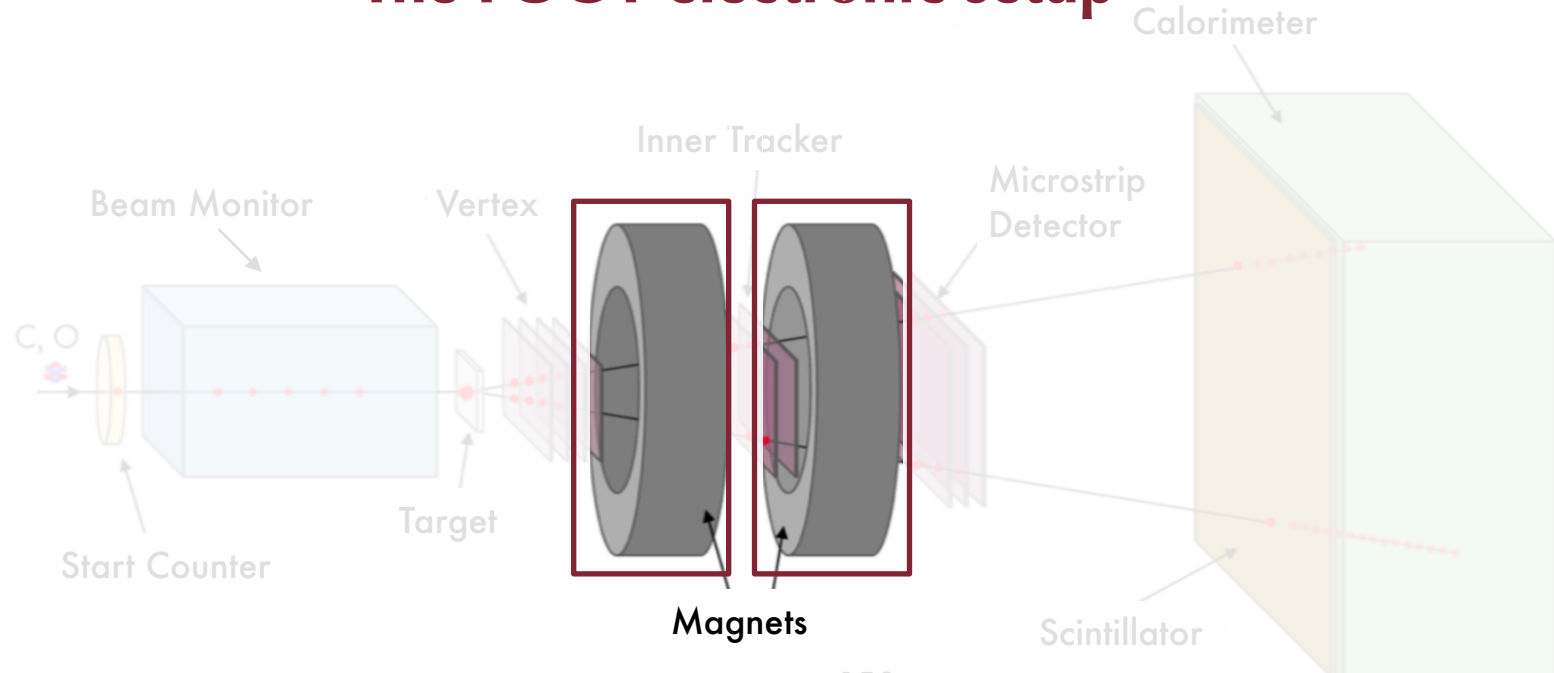
The FOOT electronic setup



Maximum rate ~ 1 kHz due to the limited readout capability (few kHz) of the tracking detectors (MIMOSA-28) and the scintillator readout that causes a delay of the order of 100 μ s

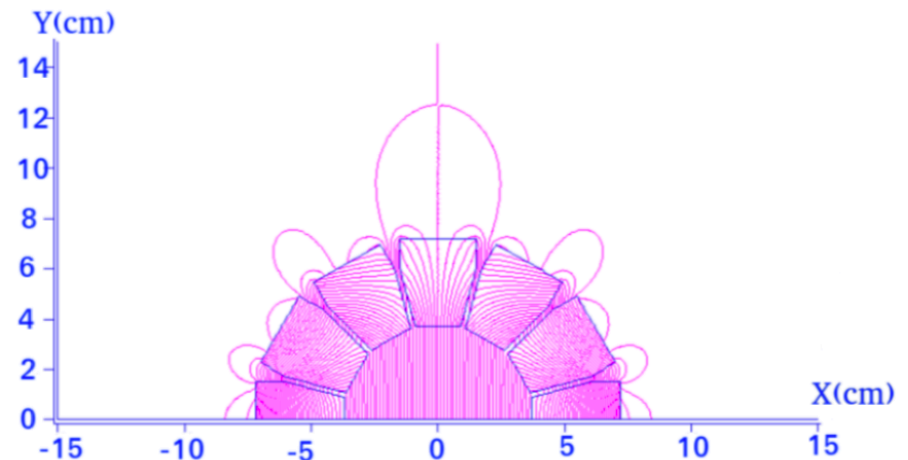
The fragments momentum is derived from the particle deflection inside the magnetic field. The tracking detectors, (VTX IT and MSD) are placed in different spots with respect to the permanent magnets in order to measure the particle position before, in the middle and after the magnetic field.

The FOOT electronic setup

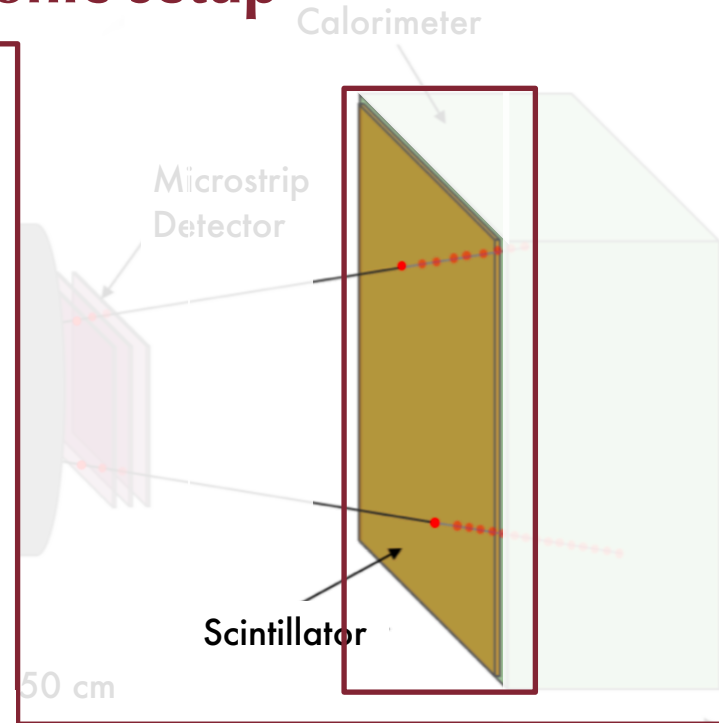
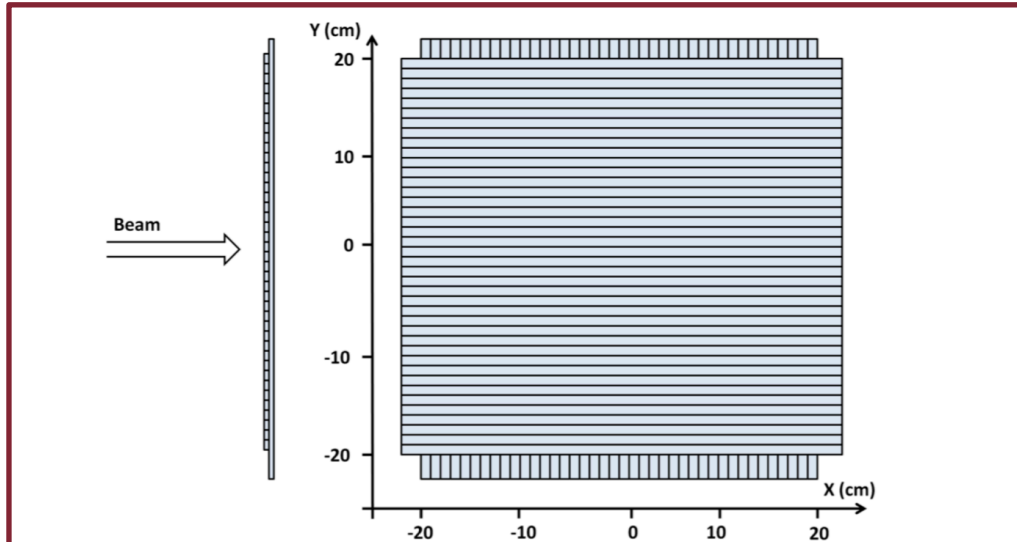


The two **Permanent Magnets** in *Halbach* configuration

- ▶ They are used to bend (~ 0.8 T) the fragments produced in the target, thus allowing their momentum identification.
- ▶ The *Halbach* configuration produces an approximately uniform field in the internal hole.



The FOOT electronic setup



The **ΔE -TOF detector** is composed by two layers of 20 orthogonally oriented plastic scintillator bars.

- ▶ Each bar, read by two SiPMs, is 3 mm thick, 2 cm wide and 44 cm long (total active area 40 x 40 cm²);
- ▶ It measures the fragments energy loss and provides the stop of the TOF measurements;
- ▶ Since the TOF is $\propto 1/\beta$, it is possible to evaluate the fragments Z using the ΔE measurements (Bethe-Bloch);
- ▶ The energy resolution is 3-5%;
- ▶ The time resolution is of the order of 40 ps (¹²C at 200 MeV/u).

Isotopic identification

When incident proton beams undergo fragmentation, they produce hydrogen, carbon or helium isotopes which, for a given kinetic energy per nucleon, have **different ranges** and so they produce **different biological damages**.

Therefore it is essential to achieve a **high accuracy on the isotopic identification (5%)** and thus on the TOF, bending and kinetic energy measurements.

The FOOT experiment aims to obtain three different estimations of the mass number:

→ β is evaluated from the TOF (<100 ns) measurements since $\beta = L/(TOF \times c)$ → TOF DETECTORS

→ p is derived from the particle deflection inside the magnetic field (5%) → TRACKERS

→ E_{kin} is the energy measured by the CALORIMETER (2-3%)

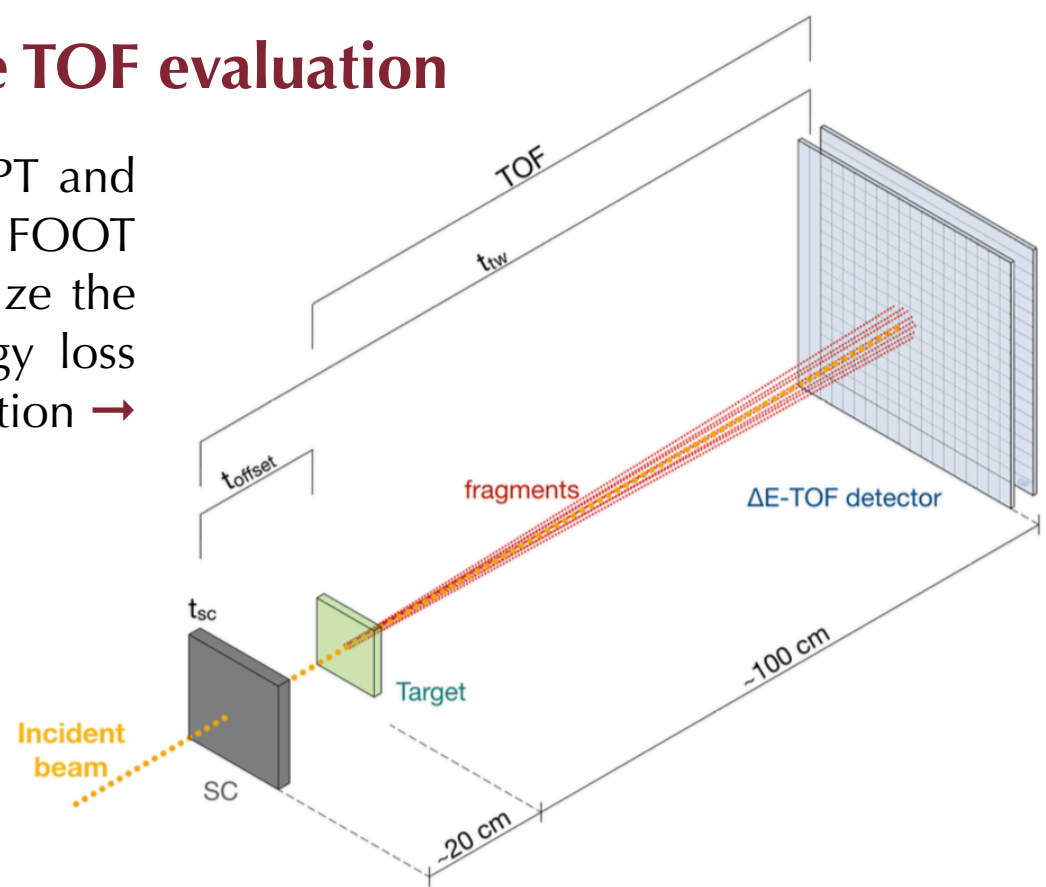
$$\begin{aligned} \triangleright A_1 &= \frac{m}{u} = \frac{1}{u} \frac{p}{\gamma \beta c} \\ \triangleright A_2 &= \frac{m}{u} = \frac{1}{u} \frac{E_{kin}}{(\gamma - 1)c^2} \\ \triangleright A_3 &= \frac{1}{u} \frac{p^2 c^2 - E_{kin}^2}{2c^2 E_{kin}} \end{aligned}$$

The TOF evaluation

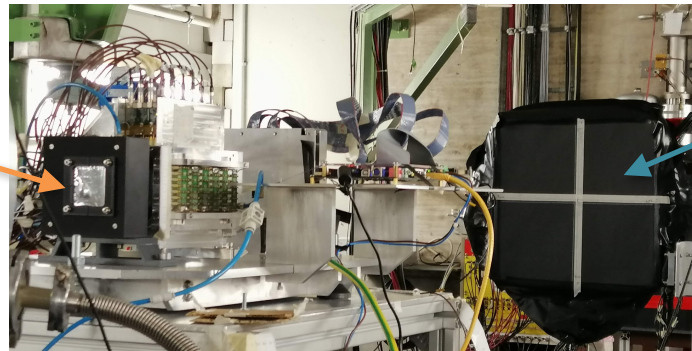
At the energy range of interest for PT and RPS applications explored by the FOOT collaboration is essential to maximize the time resolution (bending and energy loss measurements have a limited resolution → **table top experiment**).



A crucial role in minimizing the uncertainty on the isotope mass number determination is played by the fragments **Time Of Flight**.



SC detector



ΔE-TOF detector



The TOF evaluation

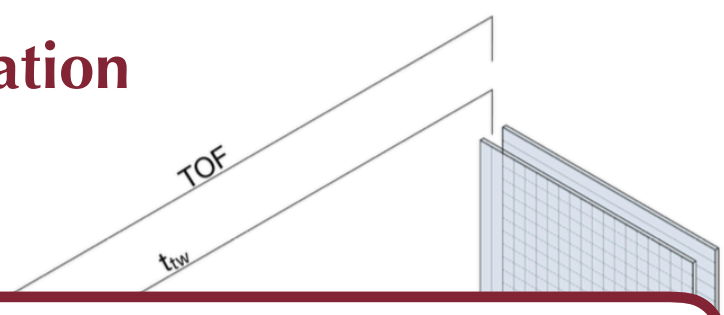
At the energy range of interest for PT and RPS applications explored by the FOOT collaboration is essential to maximize the

time
mea
tab

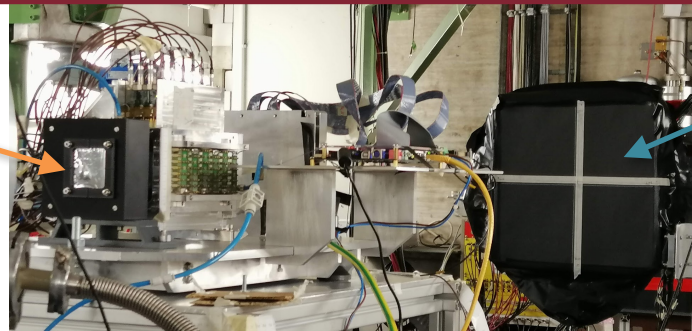
This thesis describes in detail the analysis work I have done to study the **TOF detectors performance** and **overall resolution**.

The SC is studied in detail for the **first time** in the FOOT experiment context.

I mainly focused on the **SC performance** to characterize the detector and obtain the expected **time resolution** that allows to achieve the required $\sigma(A)$



SC detector



ΔE -TOF detector

Experimental setups @CNAO

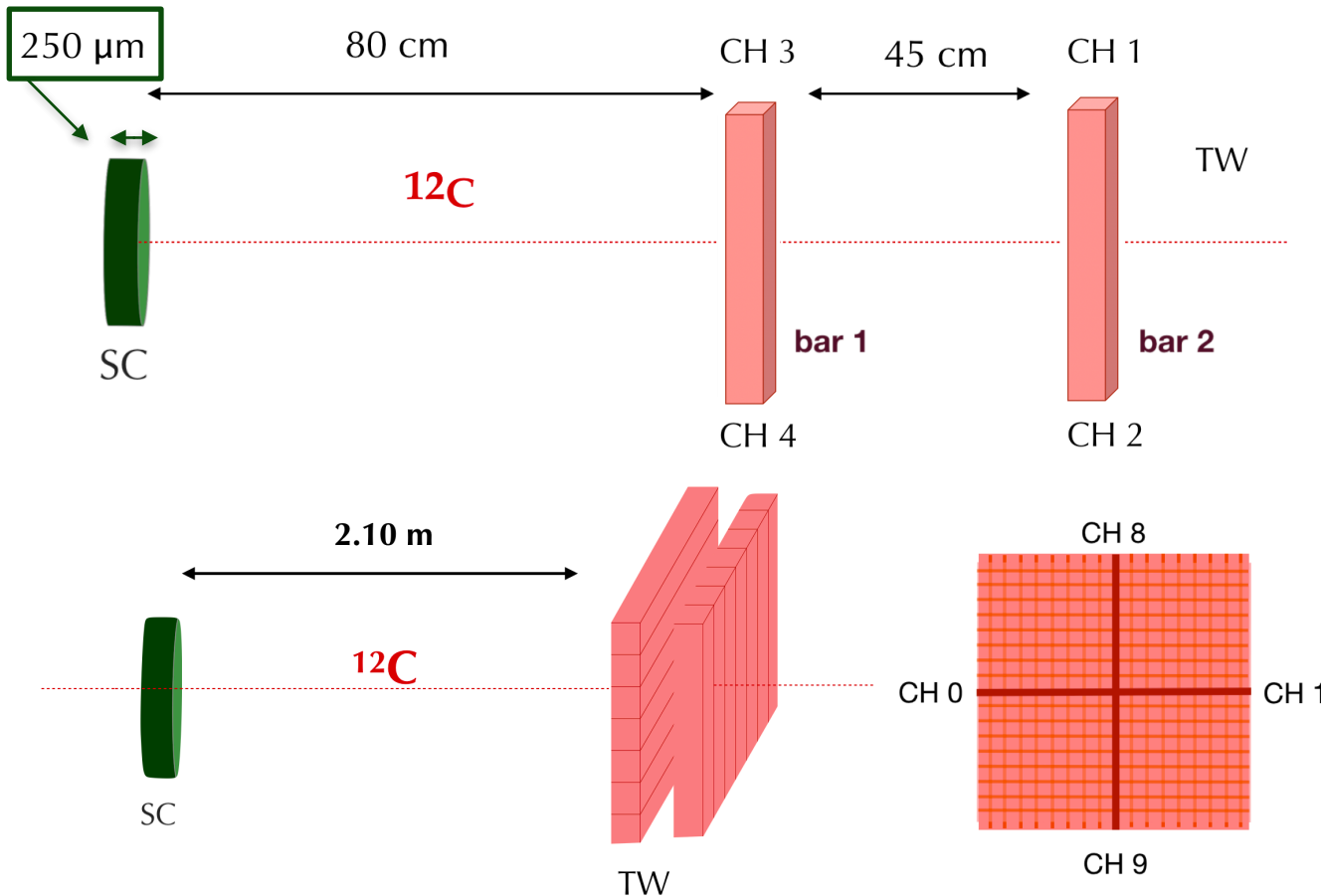
The data analyzed have been acquired using different experimental setups, testing the TOF detectors with ^{12}C and ^{16}O ions beam of different energies at CNAO (Pavia, Italy) and GSI (Darmstadt, Germany)

CNAO1

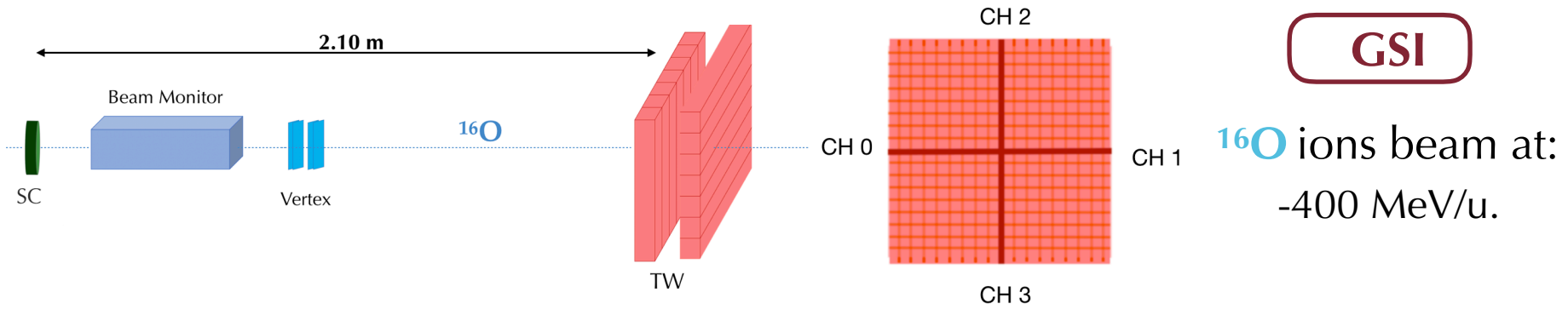
^{12}C ions beam at:
 -115 MeV/u;
 -151 MeV/u;
 -221 MeV/u;
 -280 MeV/u.

CNAO2

^{12}C ions beam at:
 -115 MeV/u;
 -260 MeV/u;
 -400 MeV/u.



Experimental setups @GSI



Since it is expected that only **5%** of the incident ions fragment inside the SC and TW and, I neglected the fragmentation contribution.

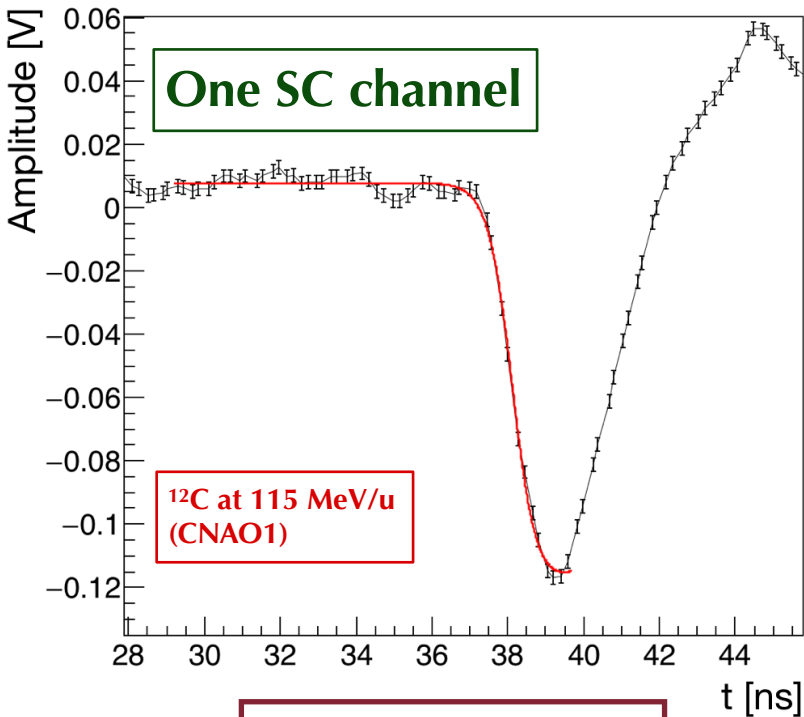
I assumed that the beam crossed the setup approximately along a straight line **without** being subjected to **deflections** or **fragmentations**.



To reconstruct the exact interaction point only two parallel bars were needed.

Arrival time evaluation

SC waveforms as measured from the digitizer (WaveDAQ system):



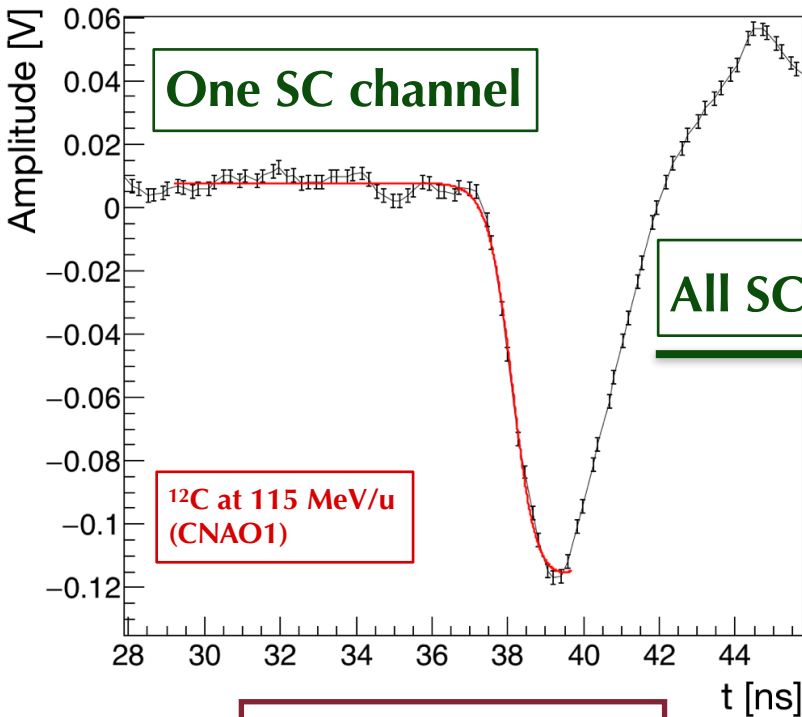
Lognormal fit
function f



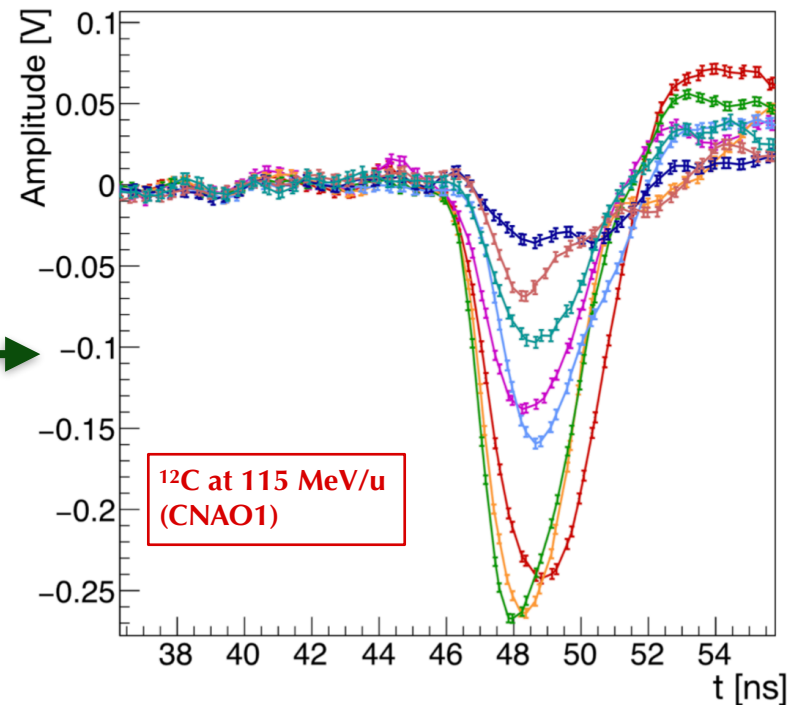
I verified the goodness of the fit
performing the χ^2 test.

Arrival time evaluation

SC waveforms as measured from the digitizer (WaveDAQ system):



All SC channels



Lognormal fit
function f

I verified the goodness of the fit
performing the χ^2 test.

To evaluate the arrival times on both SC and TW, independently of the signal amplitude, I have implemented a software algorithm capable of reproducing the **Constant Fraction Discriminator (CFD)** operation mode.

TOF evaluation

$$TOF = \bar{T}_{tw} - \bar{T}_{sc} - \Delta Clock$$

▶ $\Delta Clock$ Time jitter between the two detectors (**different electronics!**)

I have assumed that all TW bars have the same resolution and I consider only the first bar (CNAO1) and the central bar of the first layer (CNAO2-GSI).

▶
$$\bar{T}_{tw} = \frac{\sum_i T_{tw_i}}{N}$$

▶
$$\bar{T}_{sc} = \frac{\sum_i \omega_i t_{sc_i}}{\omega_i} \quad \omega_i = \frac{1}{\sigma_i^2}$$

The weights have been retrieved from the single TOF distributions:

$$TOF_i = \bar{T}_{tw} - T_{sc_i}$$

SC channels resolutions

| CH | σ [ns] | CH | σ [ns] |
|----|-------------------------------------|----|-------------------|
| 8 | 0.130 ± 0.002 | 12 | 0.170 ± 0.002 |
| 9 | 0.315 ± 0.002 | 13 | 0.119 ± 0.002 |
| 10 | <u>0.252 ± 0.002</u> | 14 | 0.115 ± 0.002 |
| 11 | 0.167 ± 0.002 | 15 | 0.117 ± 0.002 |

Different optical coupling of some SiPMs to the scintillator!!

← ^{12}C at 115 MeV/u (CNAO1)

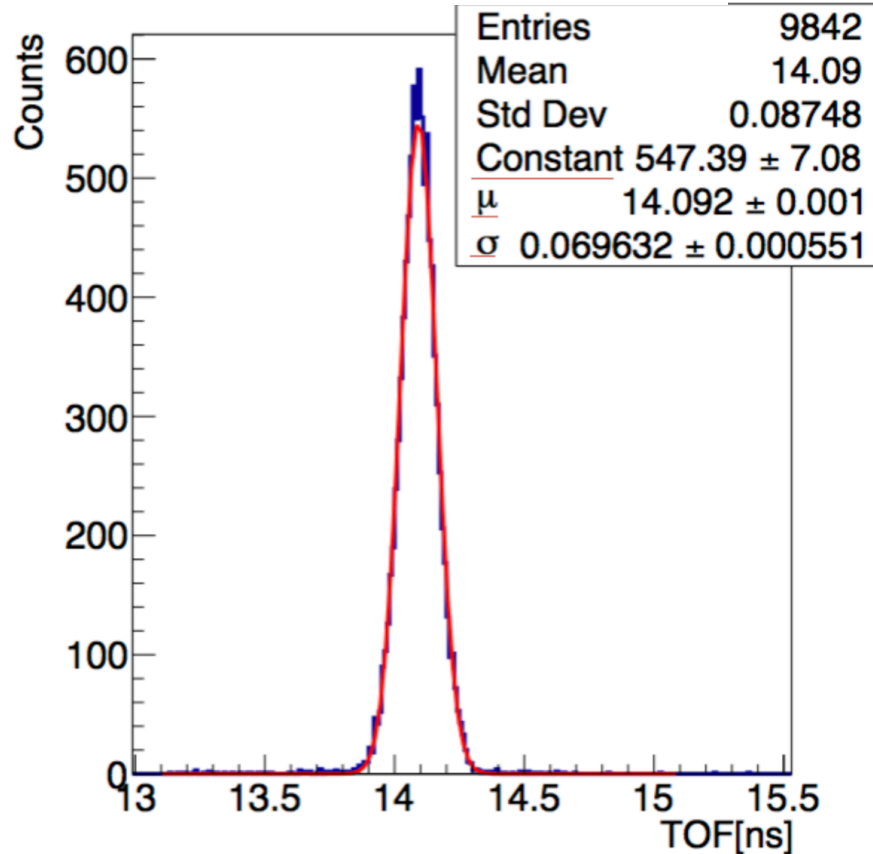
TOF evaluation

$$TOF = \bar{T}_{tw}$$

$$\bar{T}_{tw} = \frac{\sum_i T_i}{N}$$

$$\bar{T}_{sc} = \frac{\sum_i \omega_i T_{sc_i}}{\sum_i \omega_i}$$

TOF distribution



^{12}C at 115 MeV/u (CNAO1)

jitter between the detectors (**differentronics!**)

the same bar (CNAO1) NAO2-GSI).

retrieved from tions:

$$\bar{T}_i = \bar{T}_{tw} - T_{sc_i}$$

nt optical coupling SiPMs to the tor!!

5 MeV/u (CNAO1)

SC

| CH | σ [ns] |
|----|---------------|
| 8 | 0.130 ± 0.005 |
| 9 | 0.315 ± 0.005 |
| 10 | 0.252 ± 0.005 |
| 11 | 0.167 ± 0.005 |

^{12}C -CNAO1

| Energy [MeV/u] | $\sigma(TOF)$ [ps] |
|----------------|--------------------|
| 115 | 69.6 ± 0.6 |
| 151 | 73.6 ± 0.6 |
| 221 | 78.9 ± 0.7 |
| 280 | 80.1 ± 0.7 |

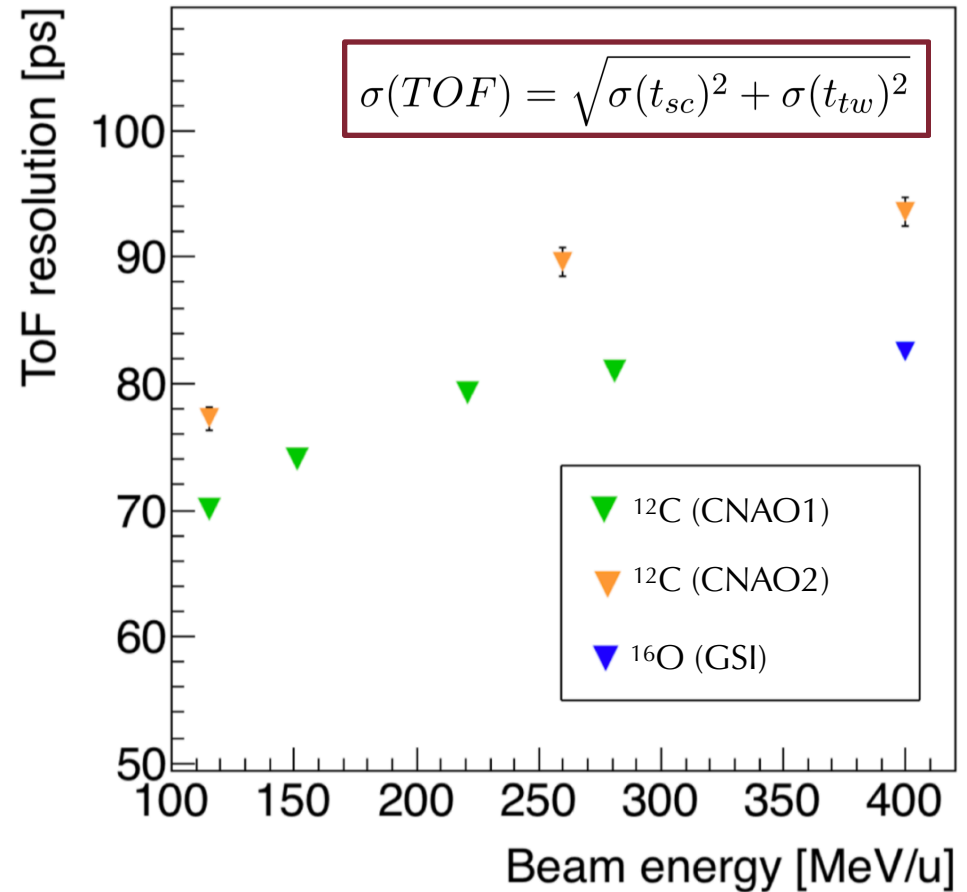
^{12}C -CNAO2

| Energy [MeV/u] | $\sigma(TOF)$ [ps] |
|----------------|--------------------|
| 115 | 76.9 ± 1.0 |
| 260 | 88.9 ± 1.1 |
| 400 | 93.2 ± 1.1 |

^{16}O -GSI

| Energy [MeV/u] | $\sigma(TOF)$ [ps] |
|----------------|--------------------|
| 400 | 82.1 ± 0.7 |

TOF resolutions



The TOF resolution for all the experimental setups follows the expected behavior:

$$\rightarrow \Delta E \propto \frac{1}{\beta^2} \propto \frac{1}{E_{kin}} \rightarrow \frac{\sigma(t)}{t} \propto \frac{1}{\sqrt{\Delta E}} \propto \sqrt{E_{kin}}$$

¹²C-CNAO1

| Energy [MeV/u] | $\sigma(TOF)$ [ps] |
|----------------|--------------------|
| 115 | 69.6 ± 0.6 |
| 151 | 73.6 ± 0.6 |
| 221 | 78.9 ± 0.7 |
| 280 | 80.1 ± 0.7 |

¹²C-CNAO2

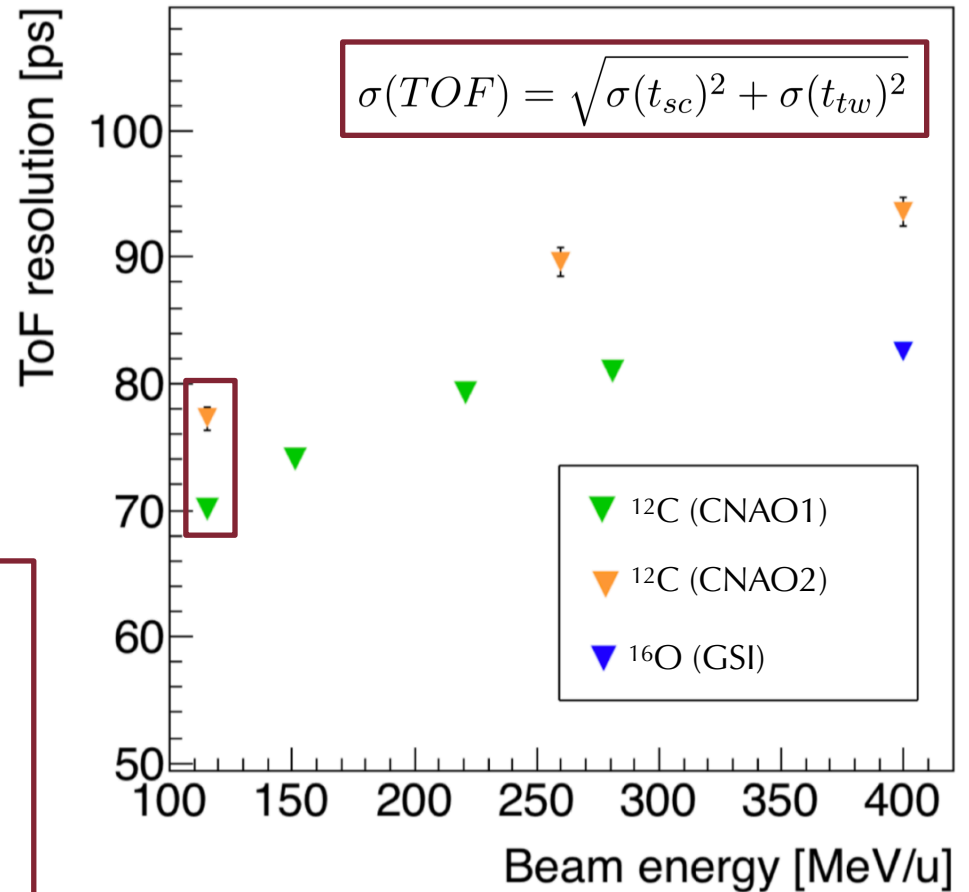
| Energy [MeV/u] | $\sigma(TOF)$ [ps] |
|----------------|--------------------|
| 115 | 76.9 ± 1.0 |
| 260 | 88.9 ± 1.1 |

The values of CNAO1 and CNAO2 data samples at 115 MeV/u have to be consistent!!

➔ This is not verified: these experimental results indicate that there is a further effect (**buffer cell correction**) that had not yet been considered (next slide)

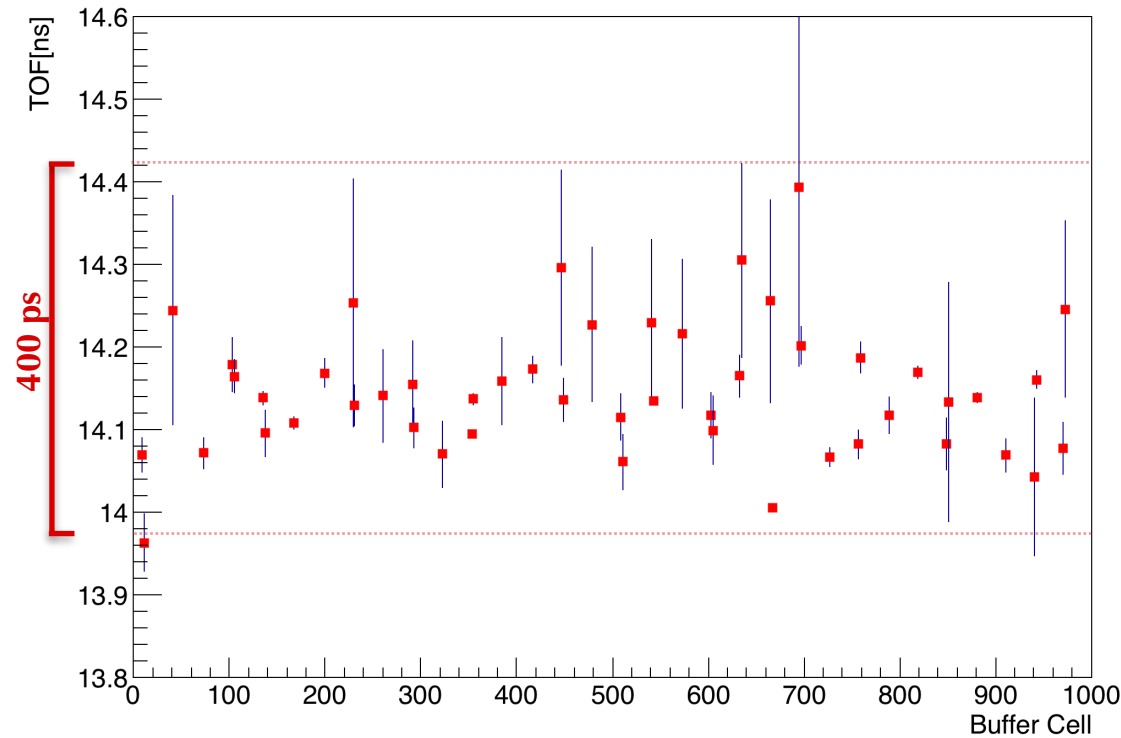
$$\rightarrow \Delta E \propto \frac{1}{\beta^2} \propto \frac{1}{E_{kin}} \rightarrow \frac{1}{t} \propto \frac{1}{\sqrt{\Delta E}} \propto \sqrt{E_{kin}}$$

TOF resolutions



tal setups follows the expected behavior:

SC channel correlation: Buffer cell correction



Since the time calibration is not uniform on all the buffer, the SC performance depends on the event **buffer cell (TC)** which is shared by its 8 channels.



Natural **correlation** that depends on the trigger cell position in the buffer.

Correction → I have decided to correct the TOF measurements according to the activated trigger cell: I have calculated, by setting a reference TC, the correction factors as the difference between the average TOF obtained for a **given buffer cell** and the one obtained for a **reference buffer cell**

$$\delta_{TC_i} = \boxed{\overline{TOF}_r} - \boxed{\overline{TOF}_i}$$



$$TOF^f = \overline{T}_{tw} - \overline{T}_{sc} - \delta_{TC_i}$$

Final TOF and SC resolutions

| | | BEFORE | |
|-----------------------------|-----------------------|--------------------|------------------------------------|
| ¹²C-CNAO1 | Energy [MeV/u] | $\sigma(TOF)$ [ps] | $\sigma(\overline{T}_{sc}^*)$ [ps] |
| | 115 MeV/u | 69.6 ± 0.6 | 68.1 ± 0.7 |
| | 151 MeV/u | 73.6 ± 0.6 | 71.6 ± 0.7 |
| | 221 MeV/u | 78.9 ± 0.7 | 73.6 ± 0.7 |
| | 280 MeV/u | 80.1 ± 0.7 | 76.9 ± 0.8 |
| ¹²C-CNAO2 | Energy [MeV/u] | $\sigma(TOF)$ [ps] | $\sigma(\overline{T}_{sc})$ [ps] |
| | 115 MeV/u | 76.9 ± 1.0 | 70.9 ± 1.2 |
| | 260 MeV/u | 88.9 ± 1.1 | 83.4 ± 1.2 |
| | 400 MeV/u | 93.2 ± 1.1 | 86.8 ± 1.2 |
| ¹⁶O-GSI | Energy [MeV/u] | $\sigma(TOF)$ [ps] | $\sigma(\overline{T}_{sc})$ [ps] |
| | 400 MeV/u | 82.1 ± 0.7 | 78.0 ± 0.7 |

The SC resolution has been retrieved according to

$$\sigma(TOF)^2 = \sigma(T_{tw})^2 + \sigma(T_{sc})^2$$

← **bar resolution**

Final TOF and SC resolutions



¹²C-CNAO1

| Energy [MeV/u] |
|----------------|
| 115 MeV/u |
| 151 MeV/u |
| 221 MeV/u |
| 280 MeV/u |

BEFORE

| $\sigma(TOF)$ [ps] | $\sigma(\bar{T}_{sc}^*)$ [ps] |
|--------------------|-------------------------------|
| 69.6 ± 0.6 | 68.1 ± 0.7 |
| 73.6 ± 0.6 | 71.6 ± 0.7 |
| 78.9 ± 0.7 | 73.6 ± 0.7 |
| 80.1 ± 0.7 | 76.9 ± 0.8 |

AFTER

| $\sigma(TOF^f)$ [ps] | $\sigma(\bar{T}_{sc}^f)$ [ps] |
|----------------------|-------------------------------|
| 64.2 ± 0.5 | 56.3 ± 0.6 |
| 68.3 ± 0.6 | 61.1 ± 0.6 |
| 73.9 ± 0.7 | 66.8 ± 0.6 |
| 76.1 ± 0.7 | 69.5 ± 0.6 |

¹²C-CNAO2

| Energy [MeV/u] |
|----------------|
| 115 MeV/u |
| 260 MeV/u |
| 400 MeV/u |

| $\sigma(TOF)$ [ps] | $\sigma(\bar{T}_{sc})$ [ps] |
|--------------------|-----------------------------|
| 76.9 ± 1.0 | 70.9 ± 1.2 |
| 88.9 ± 1.1 | 83.4 ± 1.2 |
| 93.2 ± 1.1 | 86.8 ± 1.2 |

| $\sigma(TOF^f)$ [ps] | $\sigma(\bar{T}_{sc}^f)$ [ps] |
|----------------------|-------------------------------|
| 61.5 ± 0.8 | 53.8 ± 0.9 |
| 75.1 ± 1.0 | 69.2 ± 0.9 |
| 82.5 ± 1.0 | 75.2 ± 0.9 |

¹⁶O-GSI

| Energy [MeV/u] |
|----------------|
| 400 MeV/u |

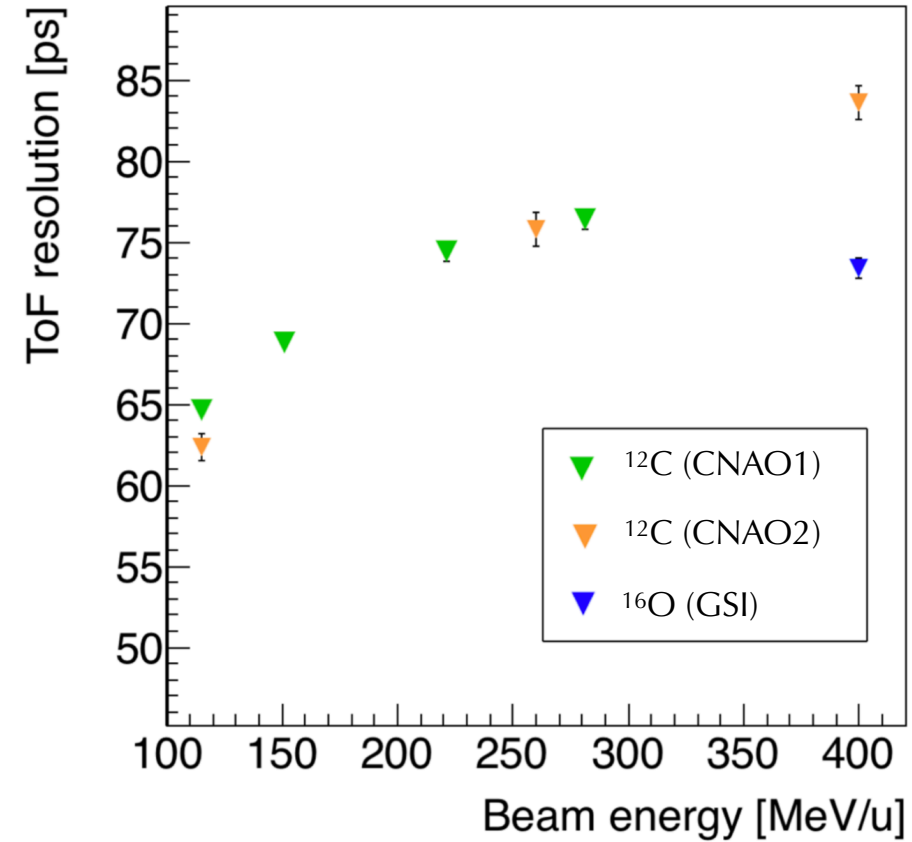
| $\sigma(TOF)$ [ps] | $\sigma(\bar{T}_{sc})$ [ps] |
|--------------------|-----------------------------|
| 82.1 ± 0.7 | 78.0 ± 0.7 |

| $\sigma(TOF^f)$ [ps] | $\sigma(\bar{T}_{sc}^f)$ [ps] |
|----------------------|-------------------------------|
| 68.5 ± 0.6 | 63.7 ± 0.6 |

The SC resolution has been retrieved according to $\sigma(TOF)^2 = \sigma(T_{tw})^2 + \sigma(T_{sc})^2$ **bar resolution**

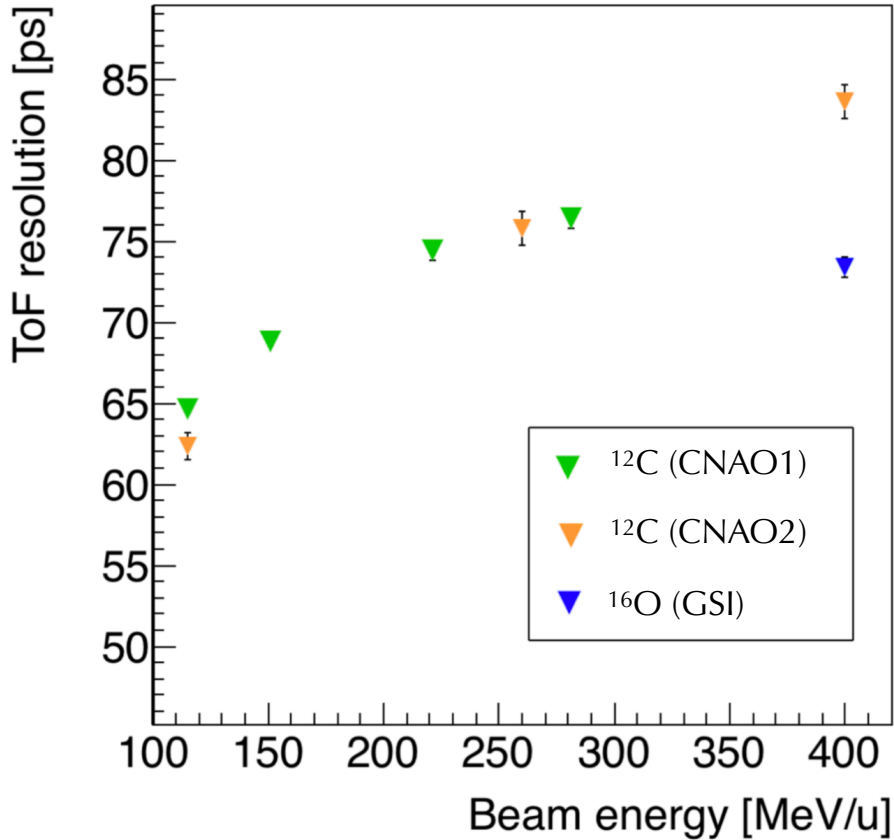
Time resolution vs Energy

TOF resolution

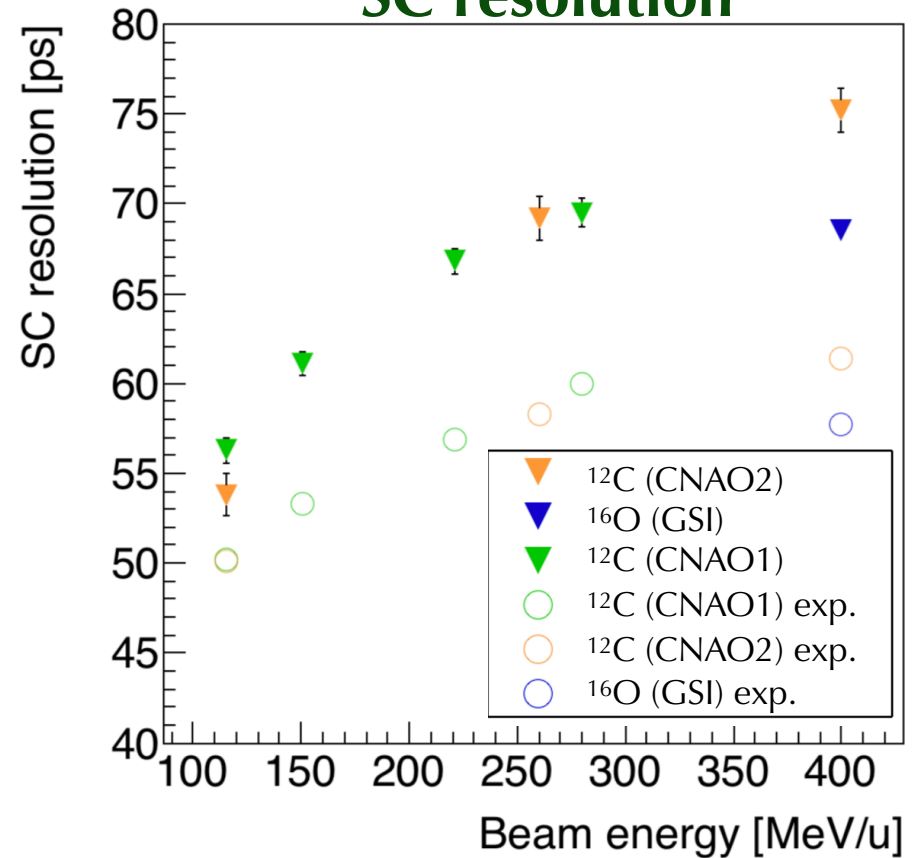


Time resolution vs Energy

TOF resolution



SC resolution



Even if the buffer cell correction has improved significantly the time resolution, the expected and measured σ values still differ. This is probably due to **the SC and TW channels correlation**.

Time resolution vs Energy

The ratio between the obtained SC time resolutions (**0.84**) of oxygen and carbon beam differs from the expected one given by:

$$\frac{\sigma(t^o)}{\sigma(t^c)} \sim \frac{Z_c}{Z_o} = 0.75$$

since $\sigma(t) \sim 1/\sqrt{\Delta E}$ where ΔE is:

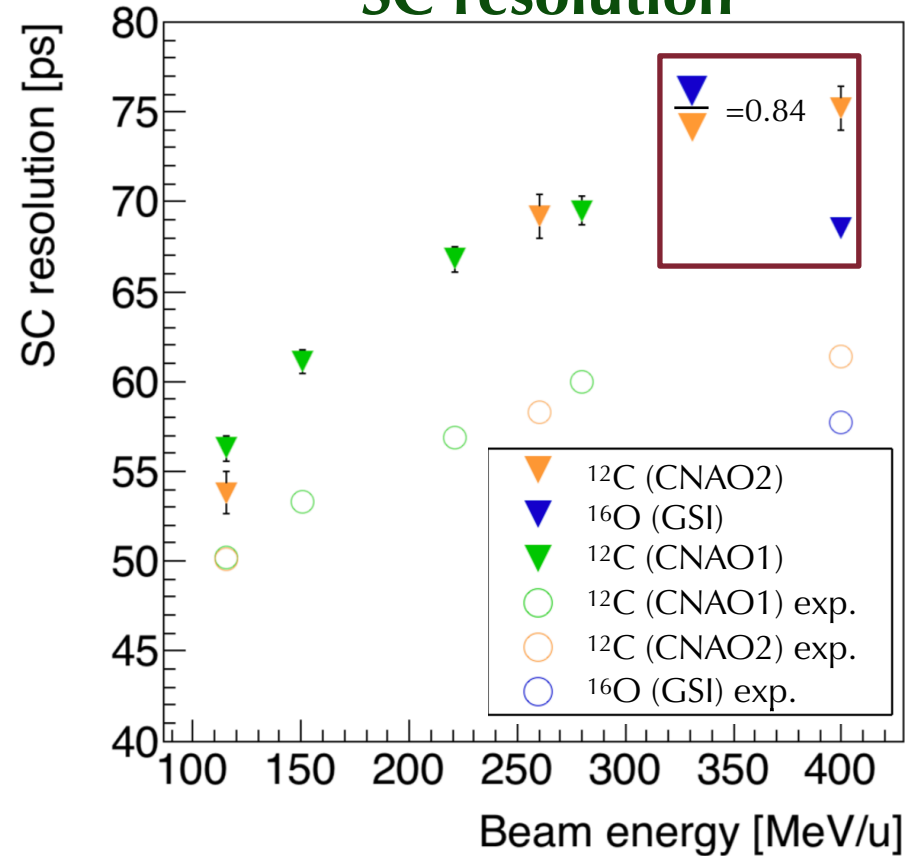
$$\Delta E \sim \frac{Z^2}{\beta^2} \sim \frac{Z^2}{E_{kin}}$$

❖ Bethe-Bloch

This discrepancy suggests that there's a systematic effect that has to be accounted for when comparing the results obtained using the carbon and oxygen data samples

➔ GSI: relevant noise superimposed to the signals in ~ 3 – 4% of the events

SC resolution



Improved significantly the time resolution, the ... This is probably due to **the SC and TW**

Conclusions

In my thesis work:

- ➔ I have performed the TOF detectors analysis obtaining the first results of the timing performances
- ➔ I have developed and fine tuned the algorithms currently used to compute the timing information of all the detectors
- ➔ The obtained results ($\sigma(\text{SC}) \sim 60\text{-}70$ ps, $\sigma(\text{TOF}) \sim 70\text{-}80$ ps) are in good agreement with the expectations and triggered some additional work on the SC implementation

The analysis algorithm that I have developed are the basis of the data analysis that will happen in 2020 using the full electronic setup

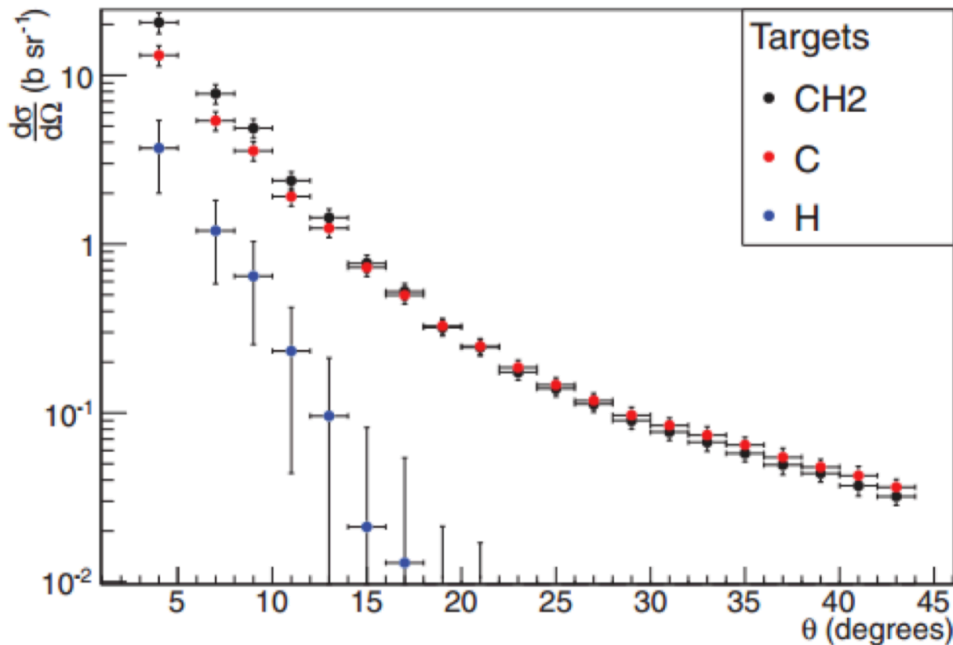


Thanks for your attention

SPARE SLIDES

Target material

Ganil: C @ 95MeV/u su C e C₂H₄



Dudouet et al., Phys.Rev.C (2013)

As a pure gaseous hydrogen target would imply the use of a specific container and thus a related systematic uncertainty

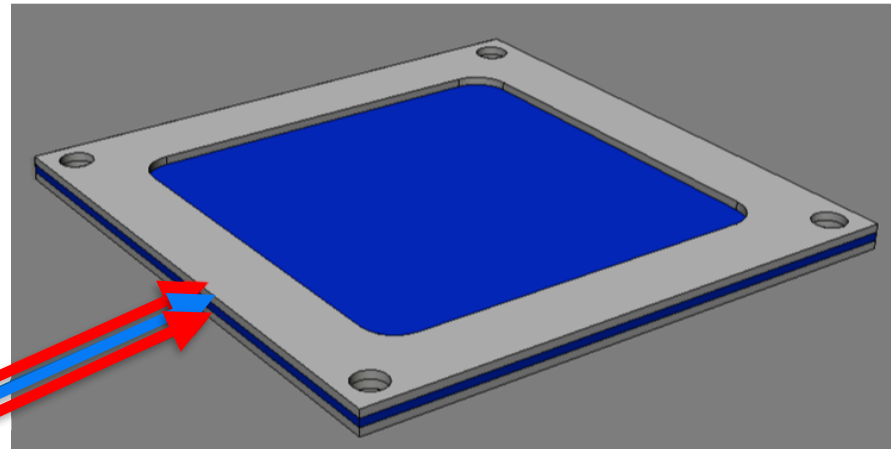


The measurements are performed with two different target: one made of carbon and the other made of an hydrogen enriched compound (C₂H₄). The hydrogen cross sections are then extracted by the data obtained with two targets.

$$\sigma(H) = \frac{1}{4} \left(\sigma(C_2H_4) - 2\sigma(C) \right)$$

Start Counter detector

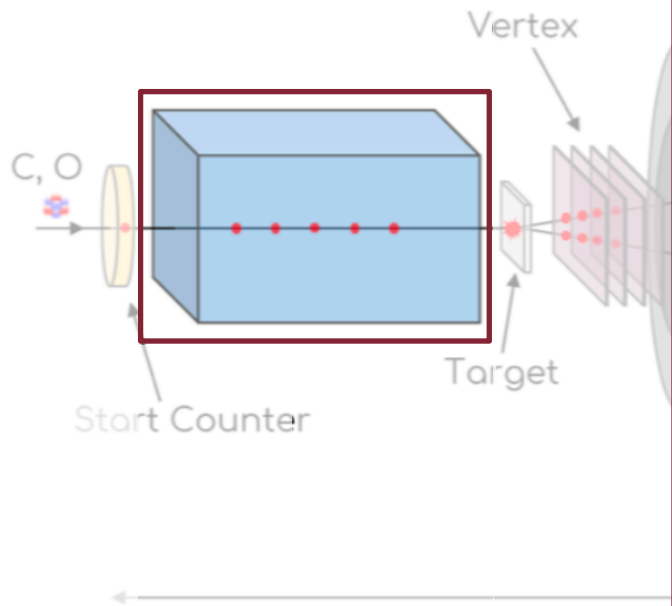
- ▶ Provides the **start** of the TOF measurements, **tigger signal** and the measurement of the **incoming ion flux** (→cross section).
- ▶ The SC aims for a time resolution **~ 70 ps** for the incoming beam particles
- ▶ Layout optimized to maximize the light collection, minimizing the out of target fragmentation probability
- ▶ Main characteristics:
 - EJ-204
 - 700 ps rise time
 - Thick: 250 μm \leftrightarrow 1 mm
 - 10 000 ph/MeV



3 mm sandwich:
1 layer 250 μm \leftrightarrow 1 mm scintillator
2 layers of 3D printed clear
(transparent) photopolymer

- ▶ The readout (8 channels) and powering of the SiPMs is handles by the WaveDREAM board.

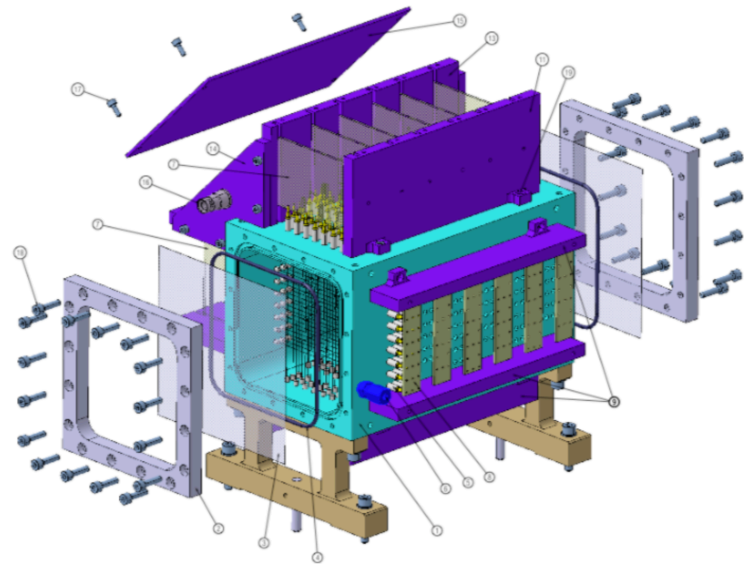
The FOOT experiment setup



Maximum rate ~ 1 kHz due to
pixel trackers (MIMOSA-28 sensor)
100 μs

The **Beam Monitor** (BM) is a drift chamber (Ar/CO₂) with a total dimension of 21x11x11 cm³.

- ▶ Its purpose is to measure the beam direction, which is essential for the Lorentz boost;
- ▶ the mean track spatial resolution is $\approx 140 \mu\text{m}$;
- ▶ the readout time is $\approx \mu\text{s}$.



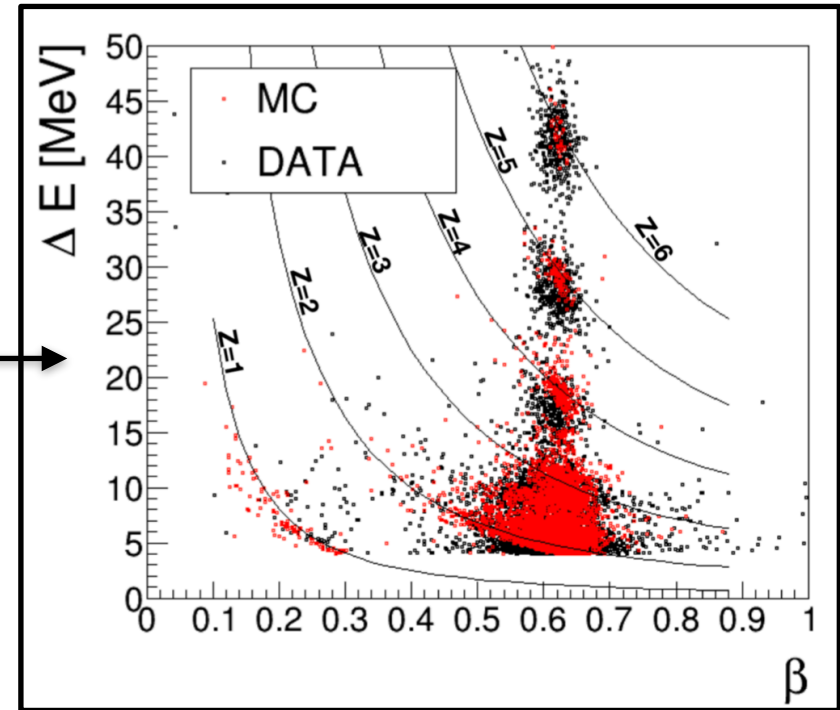
ΔE -TOF detector

► It gives the **stop** of the TOF and it contributes to the particles identification by providing the **velocity β** of the crossing fragments, which is obtained by the TOF, and the atomic number **Z**

► Main characteristic:

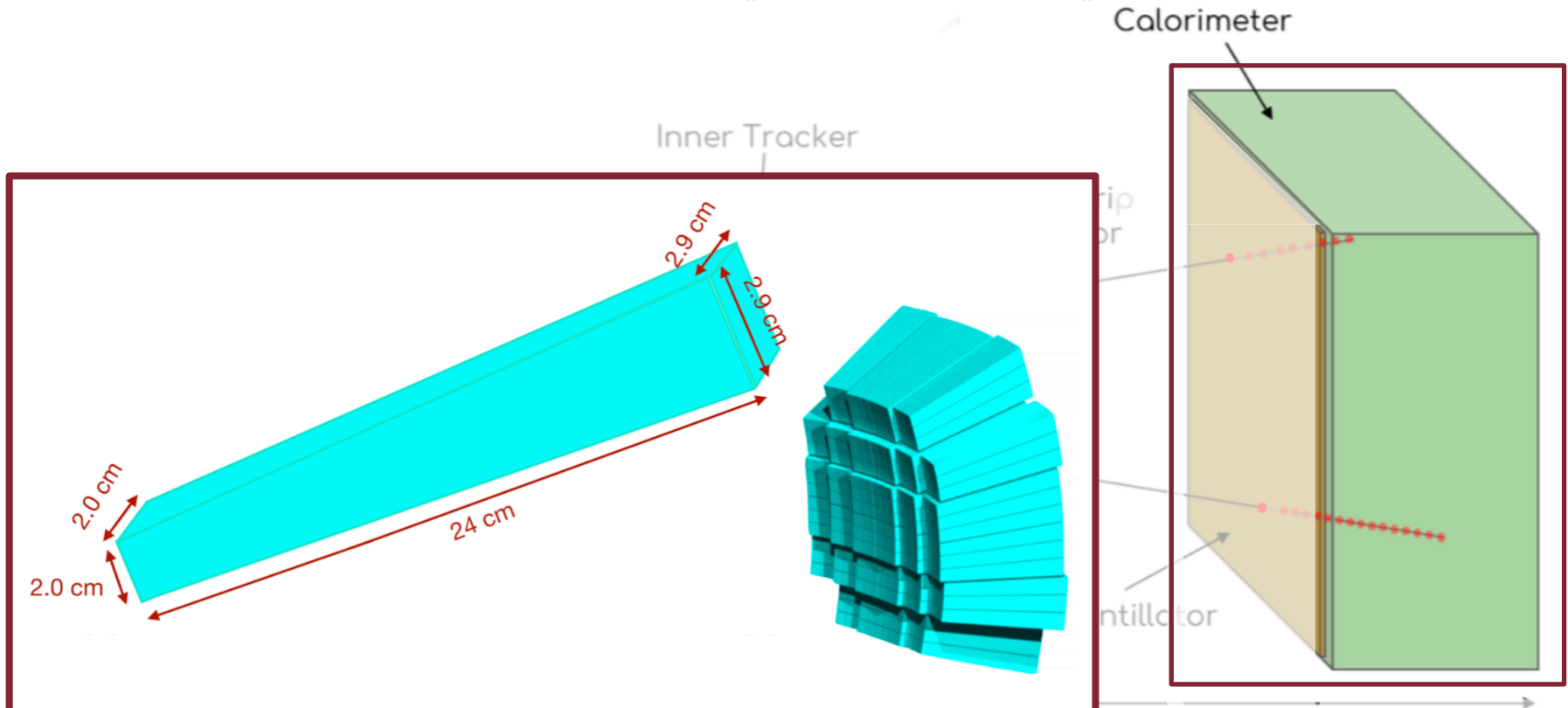
- 2 layers of 20 plastic scintillator bars (EJ-204) arranged orthogonally
- Each bar, read by two SiPMs, is 4 mm thick, 2 cm wide and 44 cm long (total active area 40 x 40 cm²)

► In order to meet the FOOT experiment final requirements, the detector should achieve resolutions **$\sigma(\Delta E)/\Delta E \sim 2-3\%$** and **$\sigma(t) \sim 40$ ns**



► The 80 signals are digitized at 5 Gsamples/s by the WaveDAQ electronics

The FOOT experiment setup

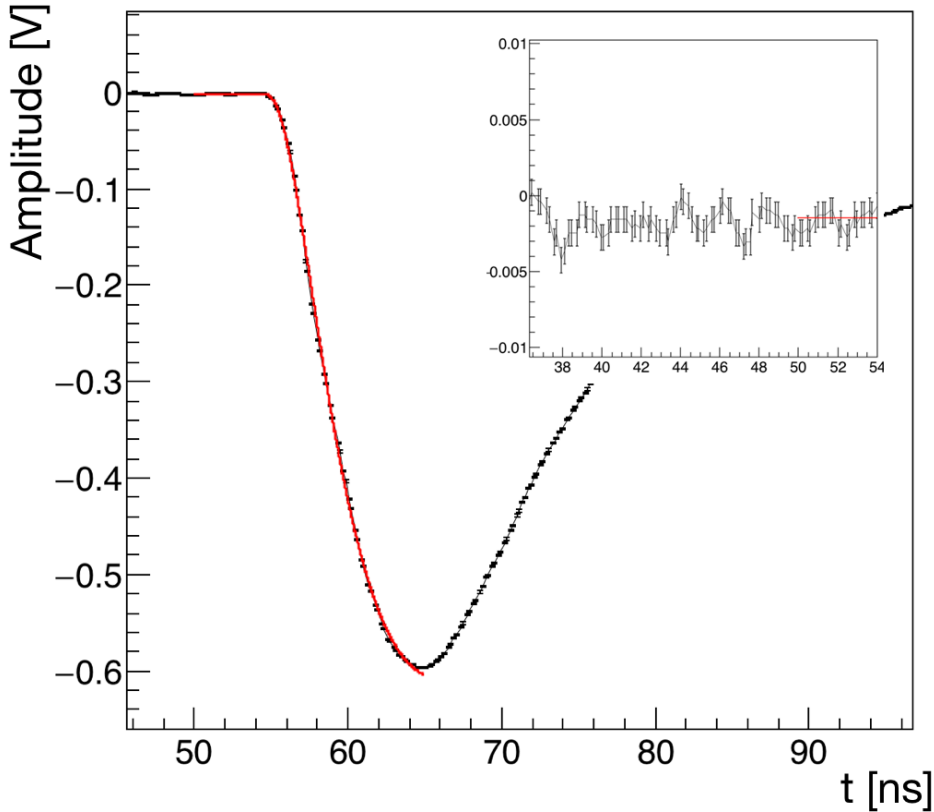


The **CALO** is composed by 288 BGO crystals with a truncated pyramid shape. These crystals are arranged in a pointing geometry.

► The expected energy resolution is between 1-3% depending on the fragment type.

(few kHz) of the silicon
ad time of the order of

TW Waveforms



Lognormal fit function f

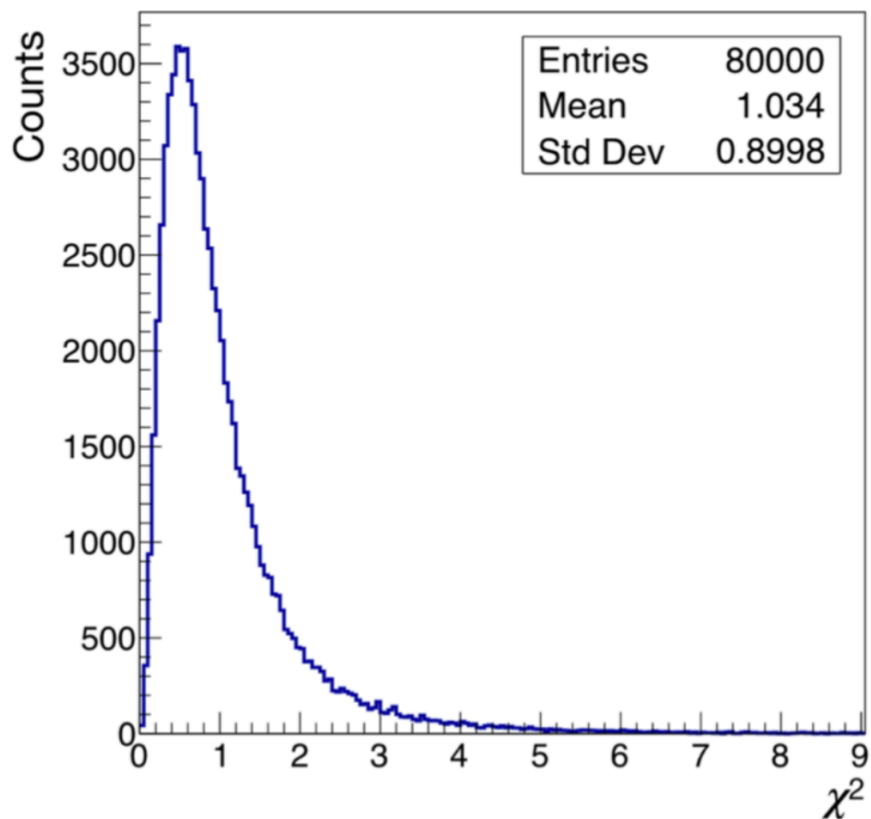
The amplitude uncertainties of all the waveforms (SC and TW) have been assigned looking at the baseline fluctuations:

TW: 0.001 V **SC:** 0.003 V

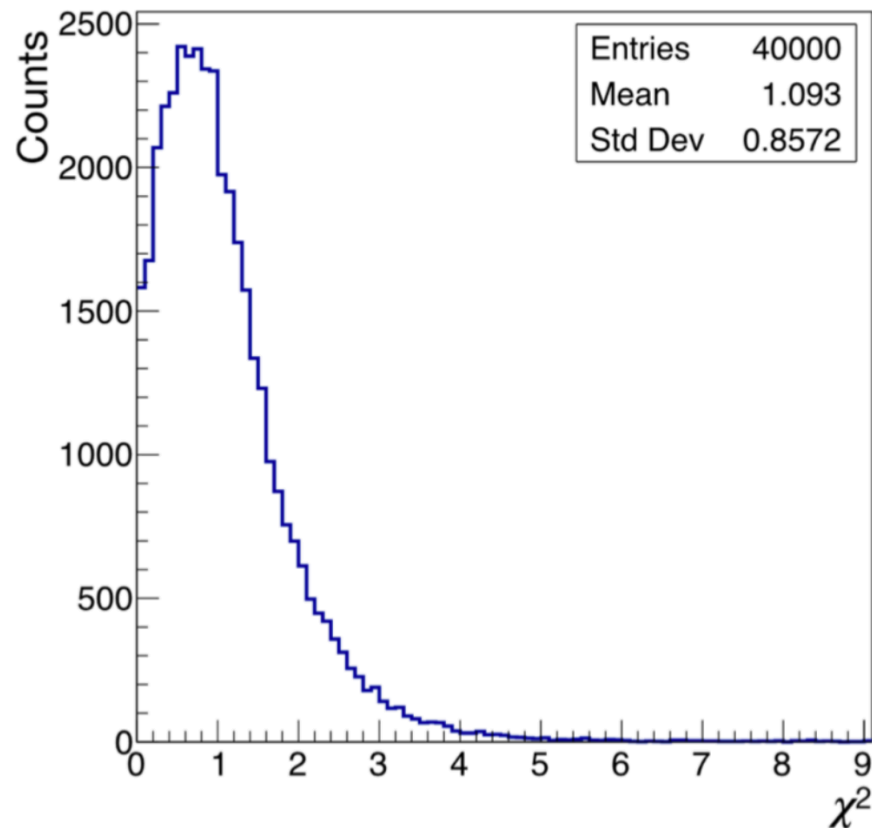
Fit goodness: χ^2 distribution

- **Waveforms fit:** lognormal fit function f

SC



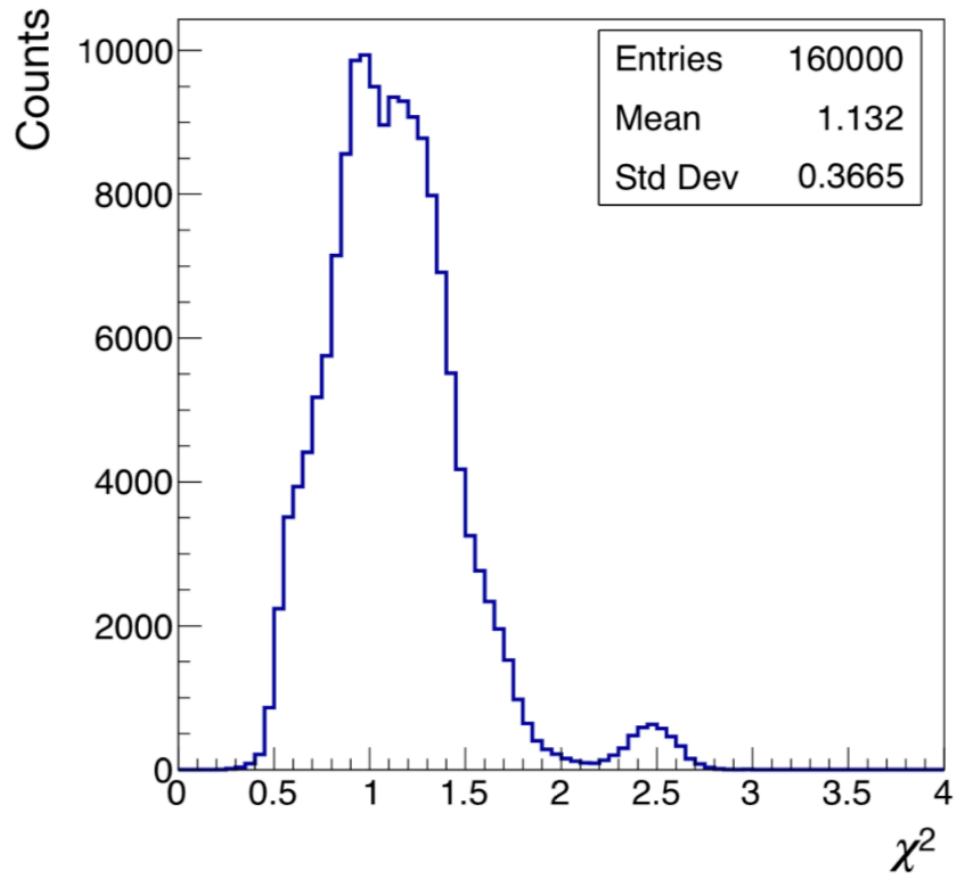
TW



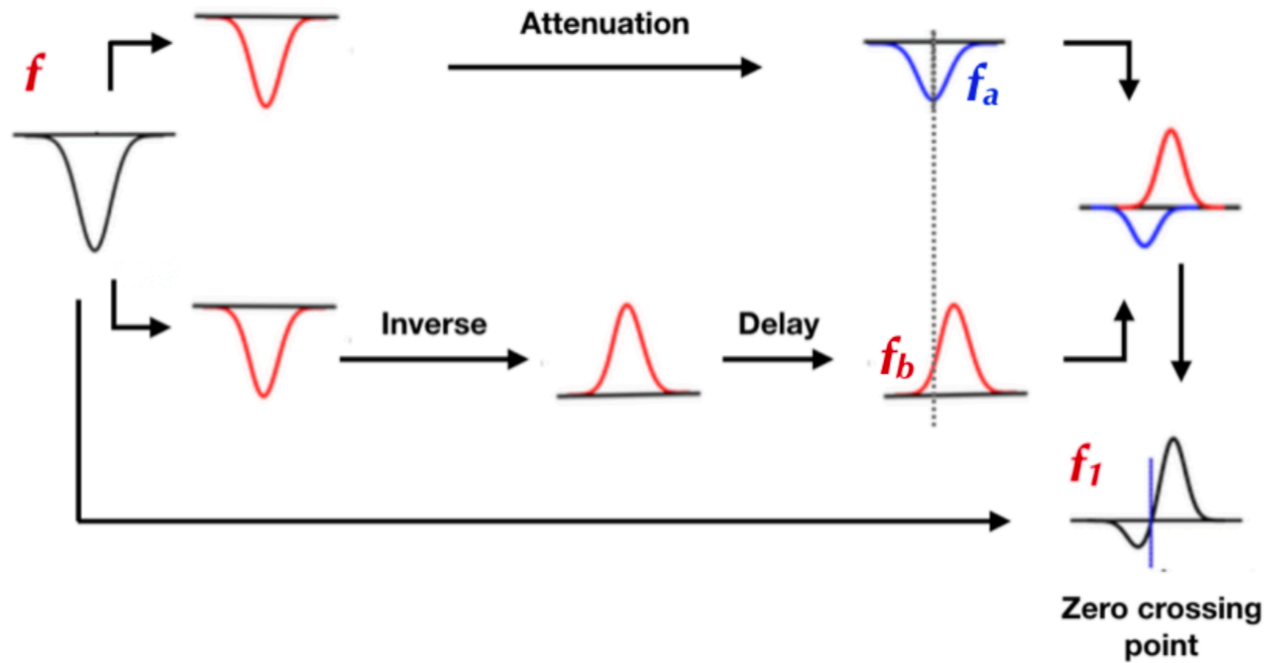
Fit goodness: χ^2 distribution

- **Clock curve fit: linear parametrization**

SC

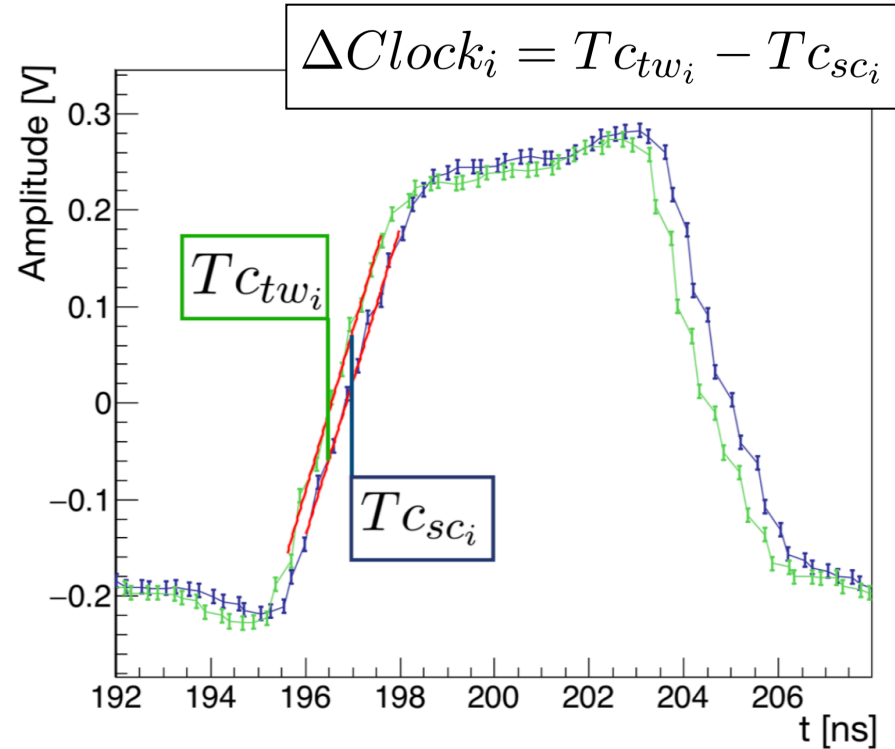
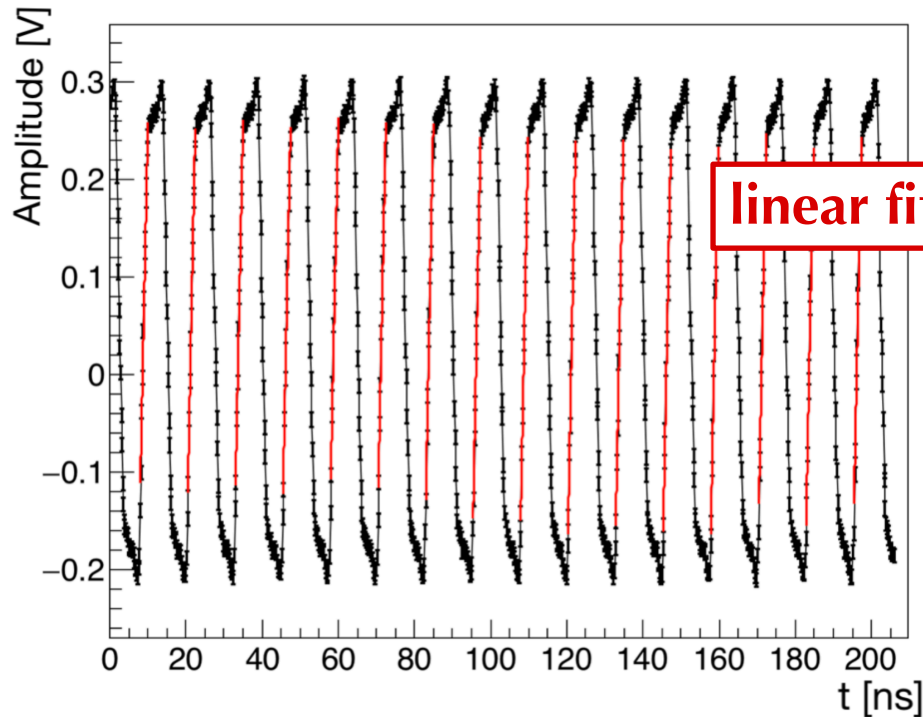


Constant Fraction Discriminator



Each signal is fitted using f . The resulting function is split into two identical parts equal to the original one. One part is attenuated to a fraction **frac** of the original amplitude obtaining f_a , and the other is inverted and then delayed by a **del** factor obtaining f_b . These two signals are subsequently added to form the constant-fraction timing signal (f_1). **The reference time then is set as the zero crossing point of the function f_1 .**

Time jitter: $\Delta Clock$ calculation



$$\overline{\Delta Clock} = \overline{T_{ctw}} - \overline{T_{csc}}$$

$$\overline{T_{ctw}} = \frac{\sum_i T_{ctw_i}}{N}$$

$$\overline{T_{csc}} = \frac{\sum_i T_{csc_i}}{N}$$

N : number of the fitted rising edges

The considered TW and SC channels belong respectively to **only** one WaveDREAM board and chip and therefore they have only **one reference clock time** each.

SC resolutions

$$\sigma(TOF)^2 = \sigma(T_{tw})^2 + \sigma(T_{sc})^2$$

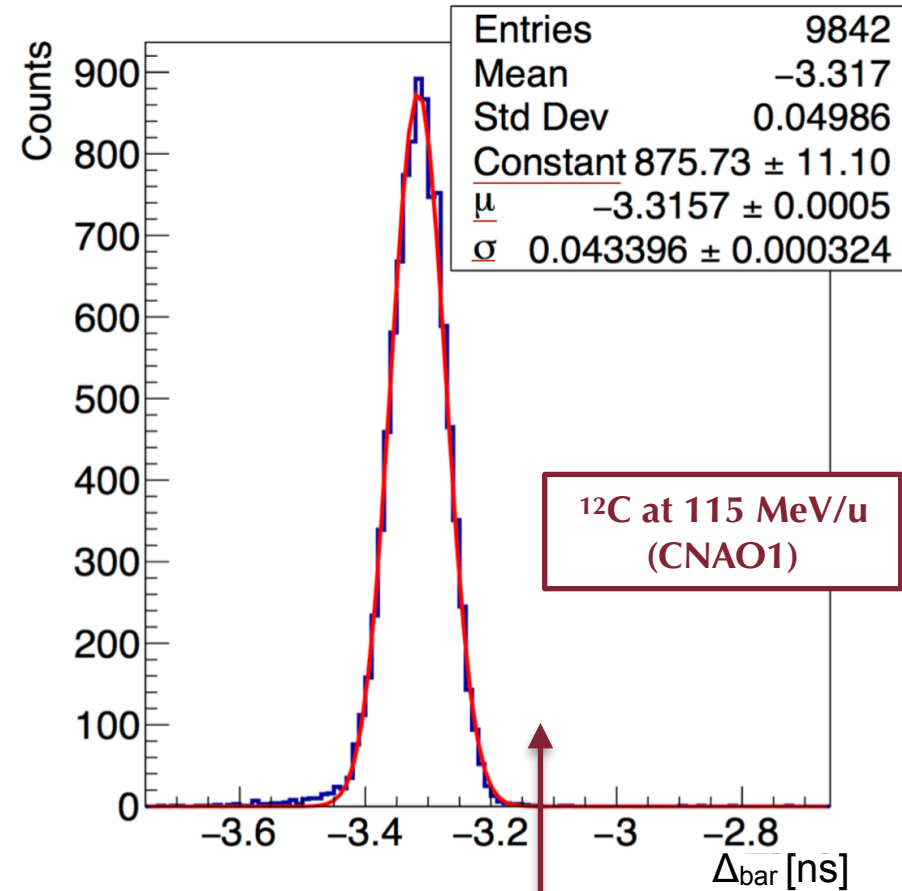
Retrieved from
the TOF
distribution

To evaluate $\sigma(T_{tw})$ I have studied the
bar resolution that can be extracted
from the distribution Δ_{bar} given by:

$$\Delta_{bar} = T_{bar_1} - T_{bar_2}$$

$$\triangleright T_{bar_1} = \frac{t_1 + t_2}{2} \quad \triangleright T_{bar_2} = \frac{t_3 + t_4}{2}$$

$$\sigma(\Delta_{bar}) = \sqrt{2}\sigma(T_{bar}) \quad \rightarrow \quad \sigma(T_{tw}) = \sigma(T_{bar}) = \frac{\sigma(\Delta_{bar})}{\sqrt{2}}$$



TW resolutions

¹²C-CNAO1

| Energy [MeV/u] | $\sigma(\overline{T}_{tw})$ [ps] |
|----------------|----------------------------------|
| 115 | 30.7 ± 0.3 |
| 151 | 30.7 ± 0.3 |
| 221 | 31.6 ± 0.3 |
| 280 | 30.8 ± 0.3 |

¹²C-CNAO2

| Energy [MeV/u] | $\sigma(\overline{T}_{tw})$ [ps] |
|----------------|----------------------------------|
| 115 | 29.8 ± 0.4 |
| 260 | 30.7 ± 0.4 |
| 400 | 34.0 ± 0.4 |

¹⁶O-GSI

| Energy [MeV/u] | $\sigma(\overline{T}_{tw})$ [ps] |
|----------------|----------------------------------|
| 400 | 25.3 ± 0.2 |

I have tested that, when comparing the data samples at 400 MeV/u of ¹⁶O and ¹²C ions, the ratio between the obtained TW time resolutions of oxygen and carbon beam (**0.74**) was comparable to the expected one given by:

$$\frac{\sigma(t^o)}{\sigma(t^c)} \sim \frac{Z_c}{Z_o} = 0.75$$

Expected SC resolutions

Based on the statistics, since the arrival time on the SC is evaluated through a weighted mean, the expected SC resolution can be retrieved as follows:

$$\sigma(\overline{T}_{tw-sc})^{ex} = \sqrt{\frac{1}{\sum_i \frac{1}{\sigma_i^2}}} \longrightarrow \sigma(\overline{T}_{sc}^{ex}) = \sqrt{(\sigma(\overline{T}_{tw-sc})^{ex})^2 - \sigma(\overline{T}_{tw})^2}$$

The σ values have been extracted from the TOF distribution measured by each SC channel (see slide n. 31):

$$TOF_i = \overline{T}_{tw} - T_{sc_i}$$

¹²C-CNAO1

| Energy [MeV/u] | $\sigma(\overline{T}_{sc})$ [ps] | $\sigma(\overline{T}_{sc}^{ex})$ [ps] |
|----------------|----------------------------------|---------------------------------------|
| 115 | 68.1 ± 0.7 | 50.2 |
| 151 | 71.6 ± 0.7 | 53.3 |
| 221 | 73.6 ± 0.7 | 56.9 |
| 280 | 76.9 ± 0.8 | 60.0 |

¹²C-CNAO2

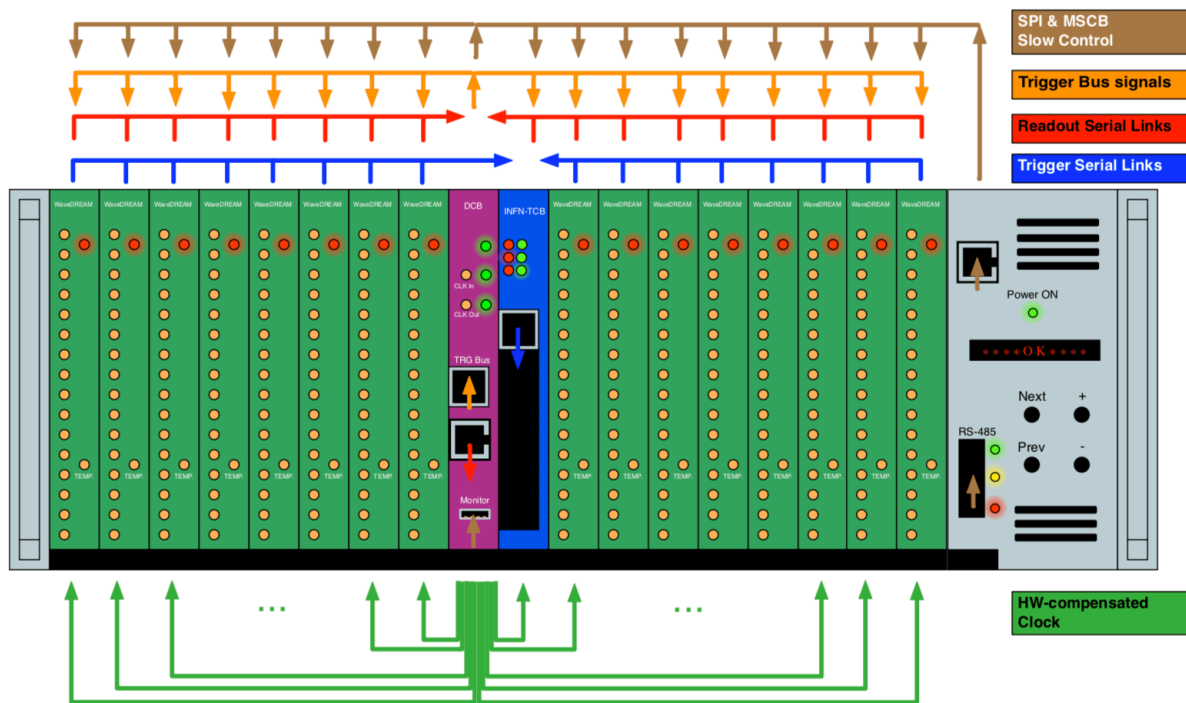
| Energy [MeV/u] | $\sigma(\overline{T}_{sc})$ [ps] | $\sigma(\overline{T}_{sc}^{ex})$ [ps] |
|----------------|----------------------------------|---------------------------------------|
| 115 | 70.9 ± 1.2 | 50.1 |
| 260 | 83.4 ± 1.2 | 58.3 |
| 400 | 86.8 ± 1.2 | 61.4 |

¹⁶O-GSI

| Energy [MeV/u] | $\sigma(\overline{T}_{sc})$ [ps] | $\sigma(\overline{T}_{sc}^{ex})$ [ps] |
|----------------|----------------------------------|---------------------------------------|
| 400 | 78.0 ± 0.7 | 57.7 |

The WaveDAQ system

One crate has 16 digitizing boards (**WaveDREAMs, WDB**) used to receive 16 inputs to be digitized by two Domino Ring Sampler (**DRS4**) chips (**one chip for 8 boards**) capable of **0.5-5 GSPS**.



► The DRS4 chip is an analog waveform digitizer composed of a chained array of 1024 cells.

When compute the particles TOF it is crucial to **synchronize** the detectors signals acquired by the channels that belong to different DRS4 chips of the same WDB or to different boards.



The clock curve of each DRS4 chip is acquired by a dedicated clock readout channel that is hence used to measure the time jitter between the detectors.